Supplementary Figure 1: Inter-individual *vs* inter-hippocampus subfields variation in gene expression.

A

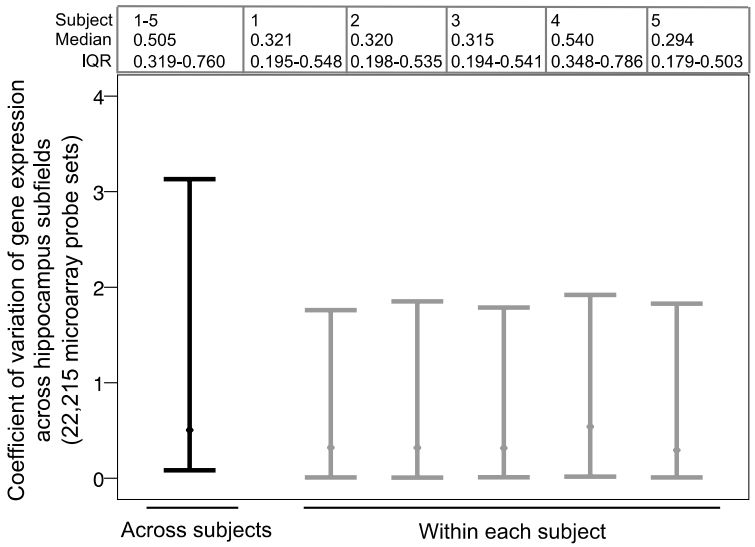

B *Functional annotation (GO terms, top and KEGG pathways, bottom) for the 518 annotated genes that were differentially expressed between the subjects (n=5)*

Top significant GO terms	Genes	Fold Enrichment	*P*-value	FDR
Defense response	56	7.7	4.1E-08	1.7E-04
Immune response	57	7.8	8.2E-07	3.1E-03
Behavior	43	5.9	1.4E-06	5.8E-03
Metal ion homeostasis	24	3.3	5.9E-06	3.2E-02
Reponse to wounding	44	6	1.4E-05	5.2E-02
Activation of phospholipase C activity	12	1.6	1.5E-05	1.4E-01
Positive regulation of phospholipase activity	12	1.6	1.5E-05	1.4E-01

Top significant KEGG pathways	Genes	Fold Enrichment	*P*-value	FDR
Neuroactive ligand-receptor interaction	34	2.6	1.2E-07	<0.1
Metabolism of xenobiotics by cytochrome P450	12	4	3.4E-05	0.19
Drug metabolism	12	3.8	4.8E-05	0.26
Cytokine-cytokine receptor interaction	28	2.1	1.1E-04	0.30
Retinol metabolism	11	4	6.1E-05	0.35
Drug metabolism	9	4.1	2.3E-04	1.40
Linoleic acid metabolism	7	4.9	3.7E-04	2.70

(**A**) We utilized surgical hippocampus samples from 5 patients with mesial temporal lobe epilepsy (MTLE) with hippocampus sclerosis (HS) of uniform pathology. For each subject, 4 hippocampus subfields were laser micro-dissected (dentate gyrus, CA1, CA3, CA4) and genome-wide expression profiles were generated for each subfield using Affymetrix HU 133A microarray. We use the coefficient of variation (CV = standard deviation/mean * 100) to quantify the degree of variation in gene expression across subfields in each subject and, after pooling together data from all subjects, the variation across subfields *and* across subjects. In each case, CV was calculated using 22,215 Affymetrix probe sets. We observed significantly bigger range of CV across subjects (black bar) than within each subject separately (grey bars). With the exception of subject 4, median and IQR of CV was higher across subjects than within each individual subject. Bars, range of the CVs; diamond, median CV. (**B**) We carried out differential expression (DE) analysis using Significance Analysis of Microarrays[1] to identify DE genes associated with (*i*) inter-individual variation and between hippocampus subfields and (*ii*) variation across hippocampus subfields only. False discovery rate (FDR) was assessed by 1,000 permutations. At 5% FDR we identified 518 DE annotated coding genes between the 5 subjects and subfields, while only 12 genes were found DE between hippocampus subfields. Functional annotation of the 518 DE genes was carried out by DAVID[2] and showed enrichment for GO terms and KEGG pathways. The results of the pilot microarray study of the hippocampus transcriptome showed higher inter-individual variability in gene expression than between hippocampus subfields within the same subject, and inform the use of whole hippocampus for subsequent genome-wide network analysis in the TLE cohort.

Supplementary Figure 2: **TLE-network genes have significant interconnectivity as compared to random Protein-Protein-Interaction (PPI) networks.**

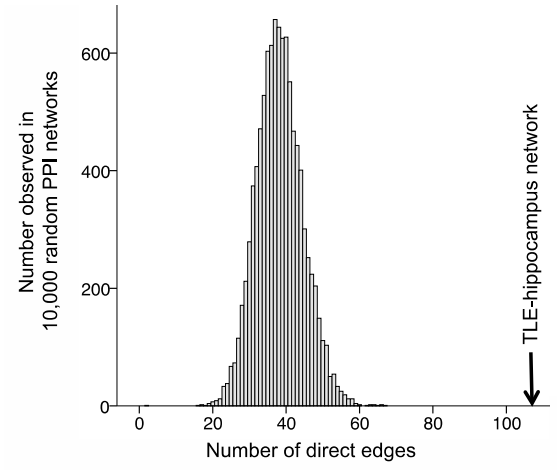

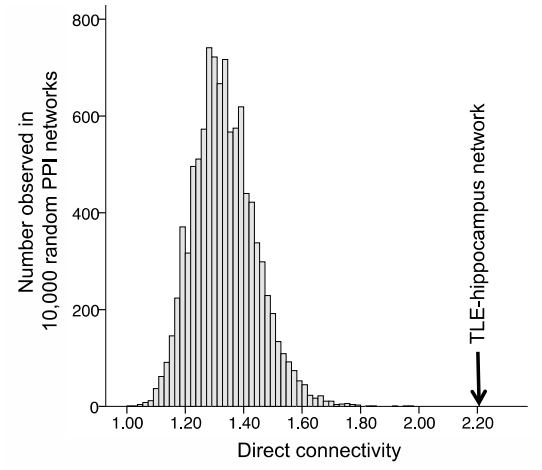

Direct PPI for TLE-hippocampus network

Direct and indirect PPI for TLE-hippocampus network

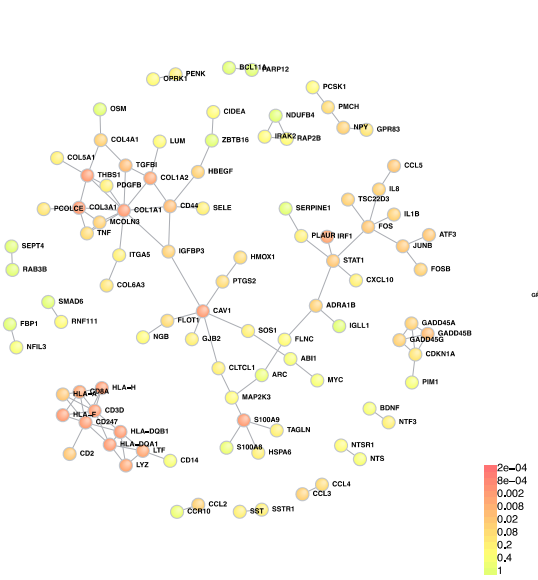

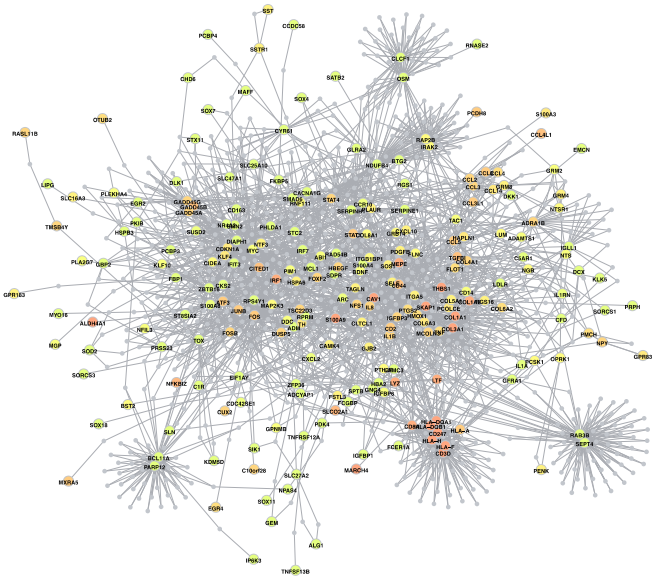

We used the DAPPLE algorithm[3] to interrogate high-confidence PPI (from InWeb database, which contains 428,430 reported interactions, 169,810 of which are deemed high-confidence, non-self interactions across 12,793 proteins) and investigated to which extent the co-regulation pattern observed at the transcriptional level (i.e., co-expression network) was conserved at the protein level (i.e., PPI). We assessed physical connections among proteins encoded for by the genes in the network identified in the hippocampus of TLE patients (TLE-hippocampus network) and tested whether these PPI are likely to be observed by chance. Looking at 10,000 random PPI networks, we found that TLE-hippocampus network genes have significantly high interconnectivity at the protein level (P = 9.9 x 10^{-5}). Histograms were plotted to represent random expectation for number of directed edges (left) and degree of direct connectivity (right); arrows indicate the number of directed edges (left) and direct connectivity (right) for the TLE-hippocampus network. The resultant PPI networks built from the TLE-hippocampus network are reported below the histograms: left, high confidence direct PPI interactions; right, global PPI network where other (indirect) PPI connected to the direct TLE-hippocampus network genes are included (grey dots). Color scale indicates the significance (P-value) of each PPI.

Supplementary Figure 3: GWAS of susceptibility to focal epilepsy.

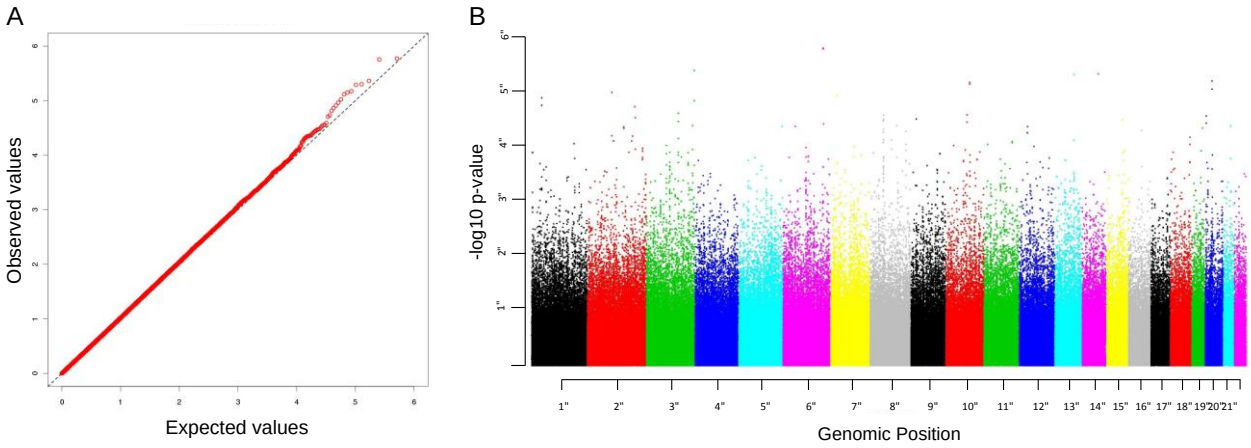

(**A**) QQ plot for focal epilepsy meta-analysis. Cases: 1,429 patients with focal epilepsy (1,013 (71%) of these had a clinical diagnosis of temporal lobe epilepsy); controls: 7,358 healthy subjects from the WTCCC2. (**B**) Manhattan plot for GWAS of focal epilepsy. All SNPs associations are reported for each chromosome, indicated by different colors. See Supplementary Methods for additional details.

Supplementary Figure 4: Comparison with gene expression from the hippocampus of healthy subjects.

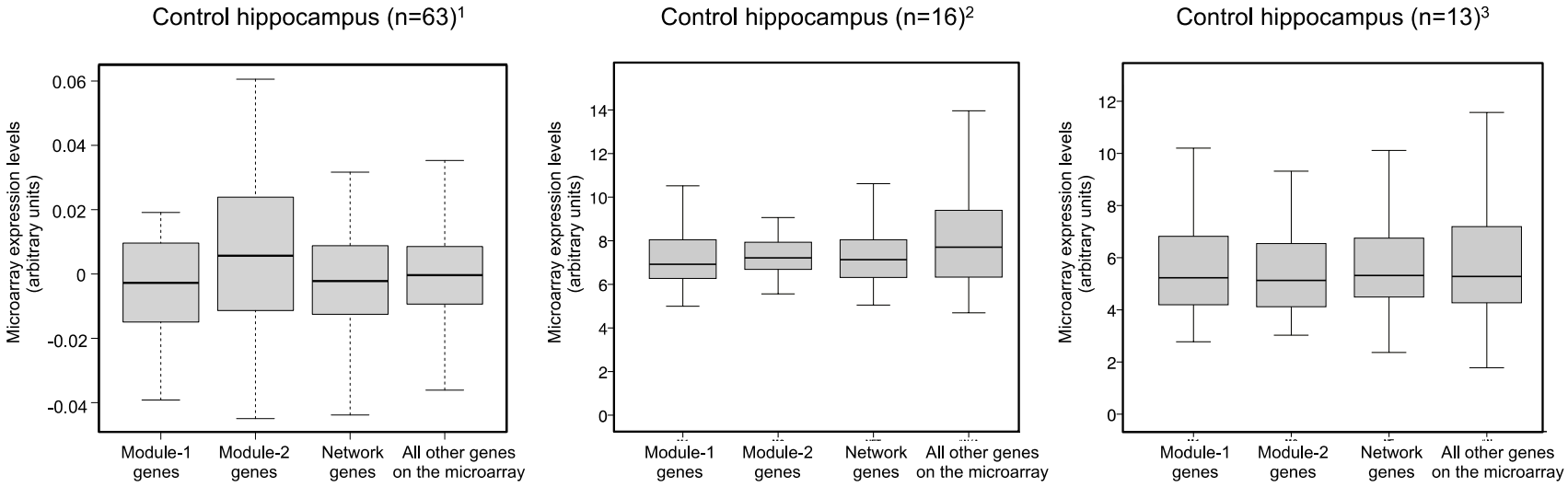

We used three separate, publicly available gene expression datasets from the hippocampus of healthy subjects and investigated whether Module-1 genes are up-regulated as compared with Module-2, the larger network or all other genes profiled by microarray. This analysis showed no significant differences between Module-1 expression and the rest of the genes analyzed, indicating that the observed up-regulation of Module-1 genes (when compared with the rest of genes analyzed, see Fig. 1e) is specific to the TLE patient cohort and it is not observed in subjects that lacked TLE (i.e., control hippocampus). A box plot-based representation of the distribution of gene expression levels for Module-1, Module-2, TLE-network and all other genes on the microarray in control hippocampi is shown below. The median, first quartile, third quartile and range in the distribution are shown.

(1) *Left panel*, hippocampal microarray expression data was obtained for 63 healthy post-mortem human brains from the Pritzker Neuropsychiatric Disorders Research Consortium; GEO accession number: GSE45642. From the whole set of gene expression data (n=670) in GSE45642, we used only 63 control samples, which had no psychiatric or neurological disorders, substance abuse, or any first-degree relative with a psychiatric disorder[4].

(2) *Middle panel*, microarray expression data form hippocampi from left and right sides of four late mid-fetal human healthy brains (18, 19, 21, and 23 weeks of gestation); GEO accession number: GSE13344.

(3) *Right panel*, microarray expression data from human hippocampal samples were collected from individuals clinically classified as neurologically normal (mean age of 79.8 ± 9.1yr); GEO accession number: GSE5281.

Supplementary Figure 5: Module-1 is enriched for TLR-signaling and cytokines.

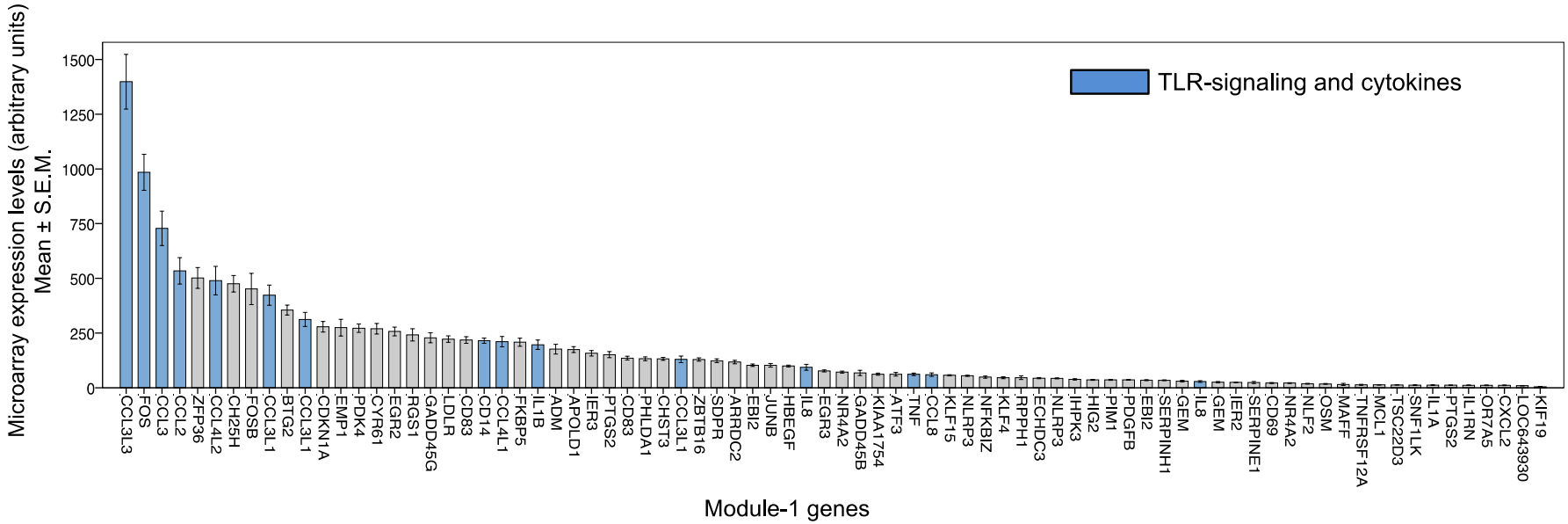

mRNA expression of Module-1 genes, showing high expression for TLR-signaling genes and cytokines (highlighted in blue). In Module-1 we found 16 fold enrichment for inflammatory cytokines (P = 6.6 x 10^{-13}), many of which belong to the IL-1 signaling cascade (*IL-1β, IL-1RN, IL-1α, TNFα*), and the TLR-signaling pathway (11 fold enrichment, P = 1.4 x 10^{-6}). Average gene expression levels (and s.e.m.) were calculated across the 129 TLE patients.

Supplementary Figure 6: Principal Component and genetic mapping analysis for Module-1 and Module-2 expression.

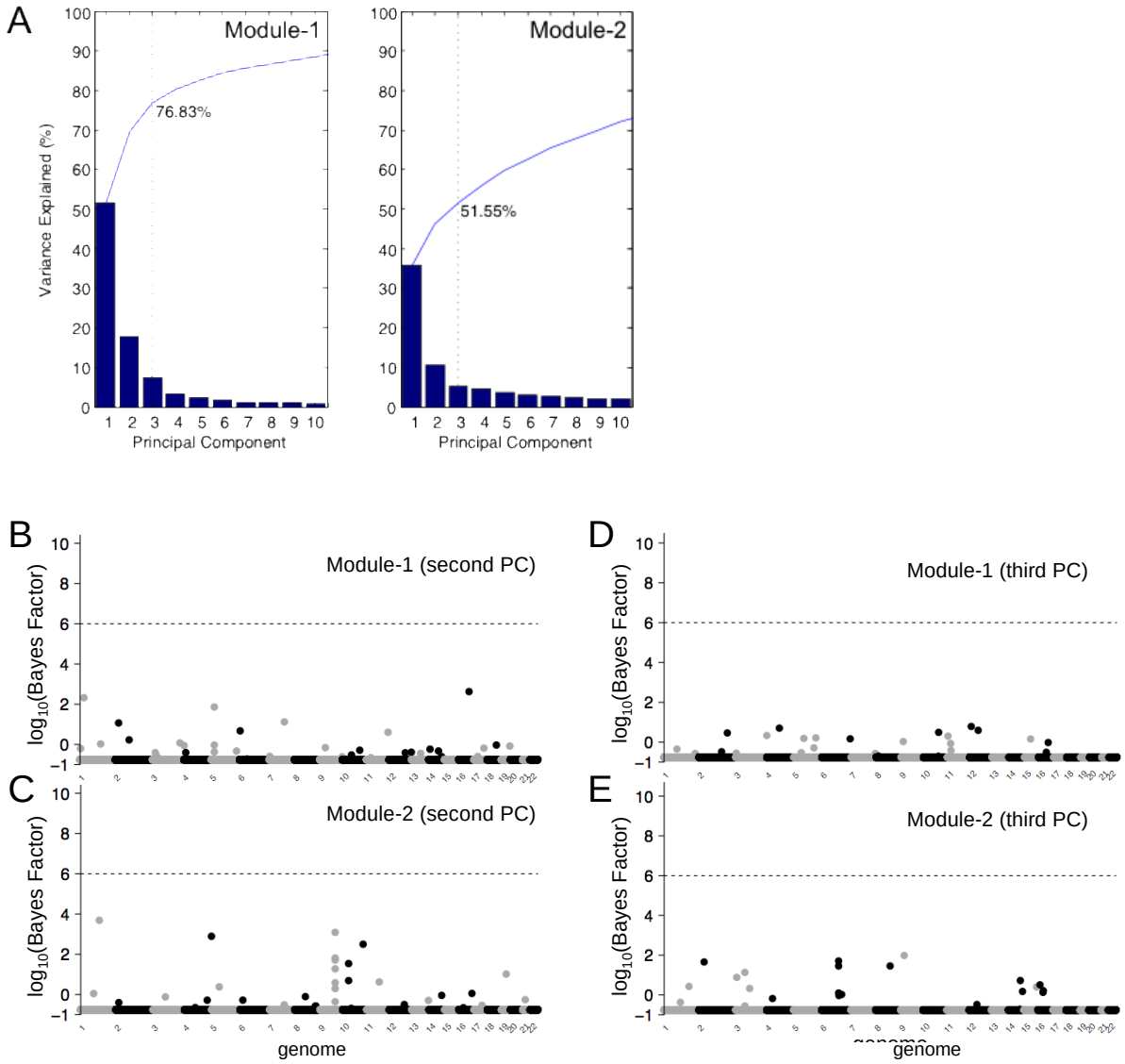

(**A**) Percentage of variance in gene expression explained by the Principal Components (PCs) for Module-1 and Module-2. For Module-1, the first three PCs accounted for ~77% of variance in gene expression, with the first PC accounting for more than half of the total variance in gene expression. For Module-2, the percentage of variance in gene expression explained the first three PCs is ~52%. Results of the genetic mapping for the second and third PC of Module-1 (**B**, **D**) and Module-2 (**C**, **E**) expression, respectively, showing no significant genetic control at local FDR<5% (i.e., $\log_{10}$(Bayes Factor) > 6). Dotted line, $\log_{10}$(Bayes Factor) = 6.

Genetic mapping results for the first PC of Module-1 expression are reported in the main text, Fig. 3a.

Supplementary Figure 7: Genome-wide correlation between *SESN3* mRNA expression and all microarray probes used for the network analysis (n=7,149).

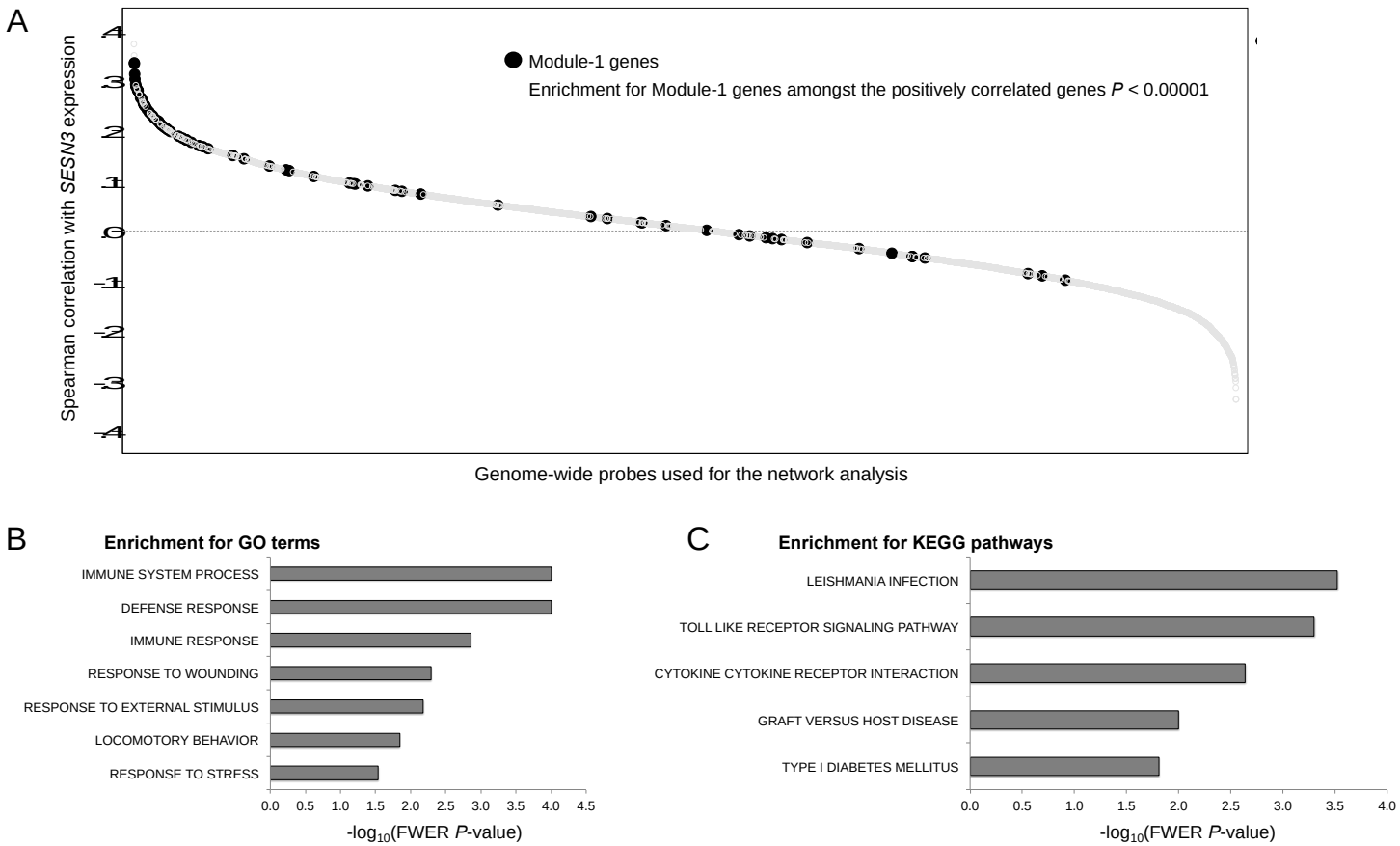

(**A**) Non-parametric Spearman correlation between *SESN3* and genome-wide probes was calculated and probe-correlations (y-axes) were ranked according to the magnitude of the correlation coefficient. The probes representing Module-1 genes are highlighted (black circles) and are significantly over-represented amongst the strongest positive correlated genes with *SESN3* expression (gene set enrichment analysis, P <0.00001). (**B**) GO terms and (**C**) KEGG pathways enrichment analysis for the most highly correlated genes with *SESN3* expression genome-wide. FWER *P*-value, family wise error rate corrected *P*-value (calculated by 10,000 permutations).

Supplementary Figure 8: Predicted regulation of Module-1 genes by activator protein 1 (AP1) transcription factor.

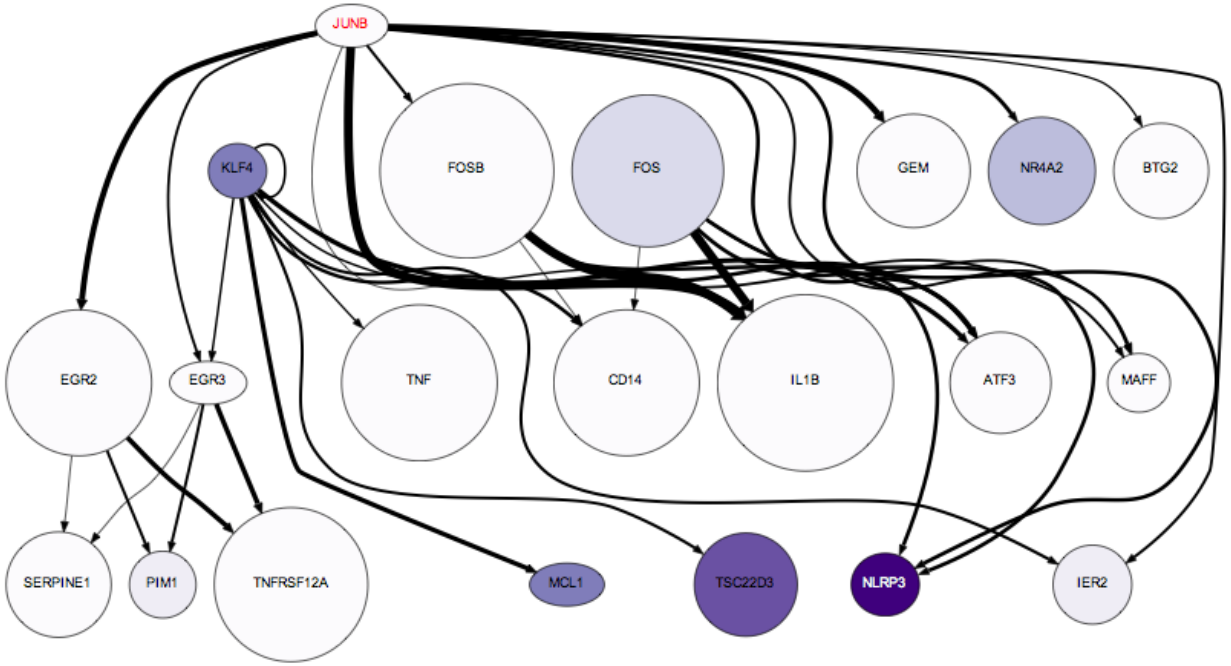

Module-1 regulation by AP1 (i.e., JUNB) was confirmed by robust transcription factor binding site (TFBS) predictions (indicated by arrowed edges in the network), which integrate physical protein-protein interaction among TFs measured using the Mammalian Two Hybrid (M2H) system and quantitative TF expression levels measured using qRT-PCR across tissues, and account for evolutionary conservation between mouse and humans (FANTOM4)[5]. AP1 is predicted to regulate, directly or indirectly, 20 genes of Module-1, and the TFBS are conserved between mouse and human. Evolutionarily conserved TFBS were predicted using the MotEvo algorithm with a set of non-redundant matrices (combining JASPAR, TRANSFAC and a small set of de-novo motifs trained on ChIP-chip datasets) and are represented as TFBS edges in the network. The weights of the TFBS edges are proportional to the "response values", which represent how well the expression of each promoter responds to the motif activity for that TF. The diameter of each node is scaled to indicate the 'dynamics' of the gene and it is calculated by mapping to log(max(detected expression)/min(detected expression)) within the time course; highly dynamic nodes are larger than statically expressed nodes. The color of the node is mapped to a relative scale for each node between white for min(detected expression) and purple max(detected expression). Arrowheads indicate activating relationship.

Supplementary Figure 9: Immunohistochemical analyses of SESN3 in human hippocampal tissue.

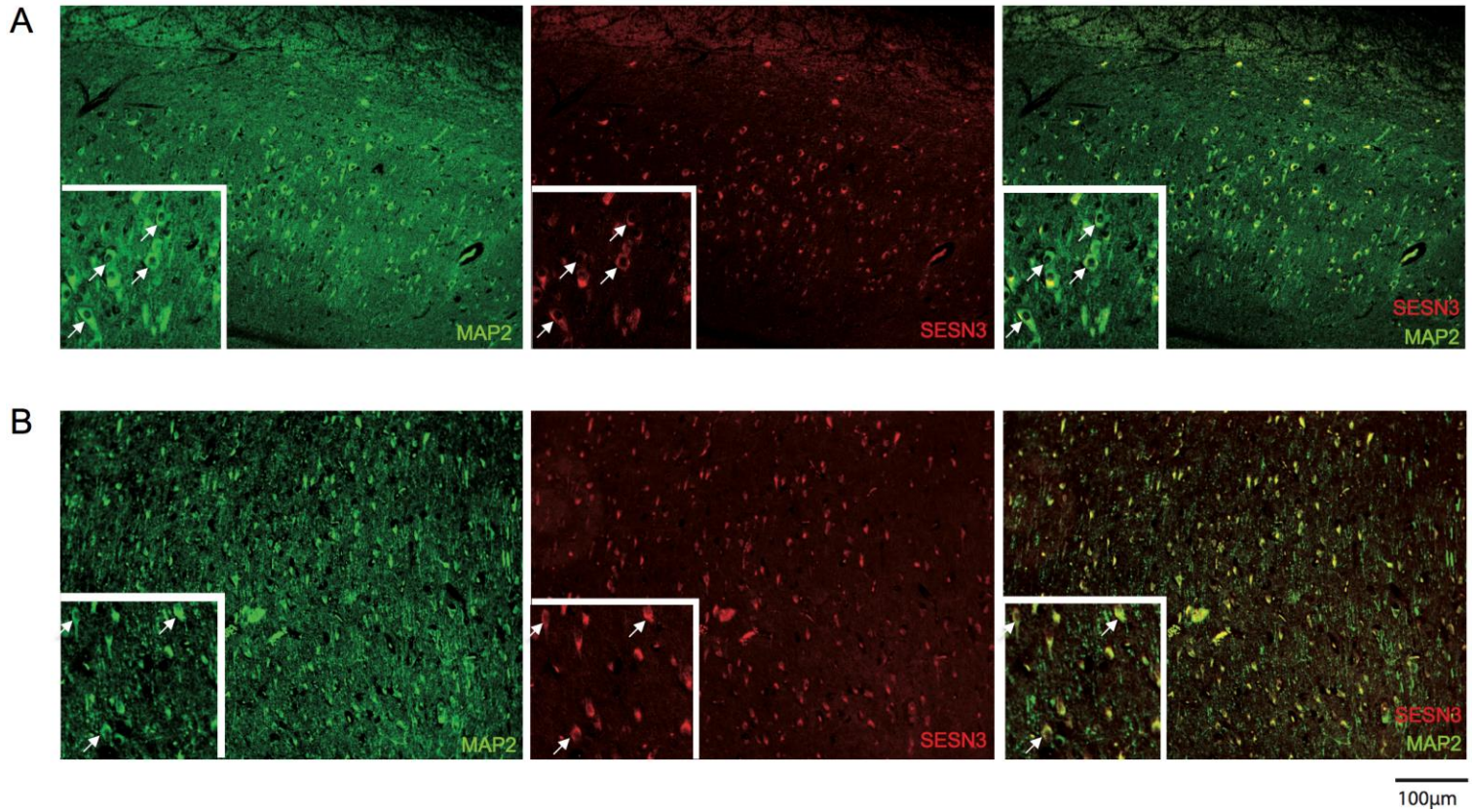

Representative images of co-immunoreactions against MAP2 (green) antibody showed that SESN3 (red) is localized in neurons in human hippocampal tissue from an autopsy specimen (**A**) and a biopsy TLE hippocampus (**B**). While several factors (e.g., time interval between tissue harvesting and fixation, post-harvesting delay, etc.) might have affected the preservation and quality of tissues samples used for immunohistochemical analyses, we observed that the number of well-defined neuronal cell bodies (MAP2 positive with central round nucleus, indicated by the white arrows below) in (**B**) is reduced, probably due to epilepsy-associated neuronal degeneration in the TLE hippocampus. Although the number of viable neurons is reduced in the TLE hippocampus, more elements showed robust expression of SESN3 – insert in the overlay (insert = 50µm). Please refer to Fig. 4e for quantification of SESN3 expression in human hippocampal tissue by immunofluorescence analysis.

Supplementary Figure 10: **Up-regulation of *Sesn3* gene expression in the mouse hippocampus after pilocarpine-induced status epilepticus.**

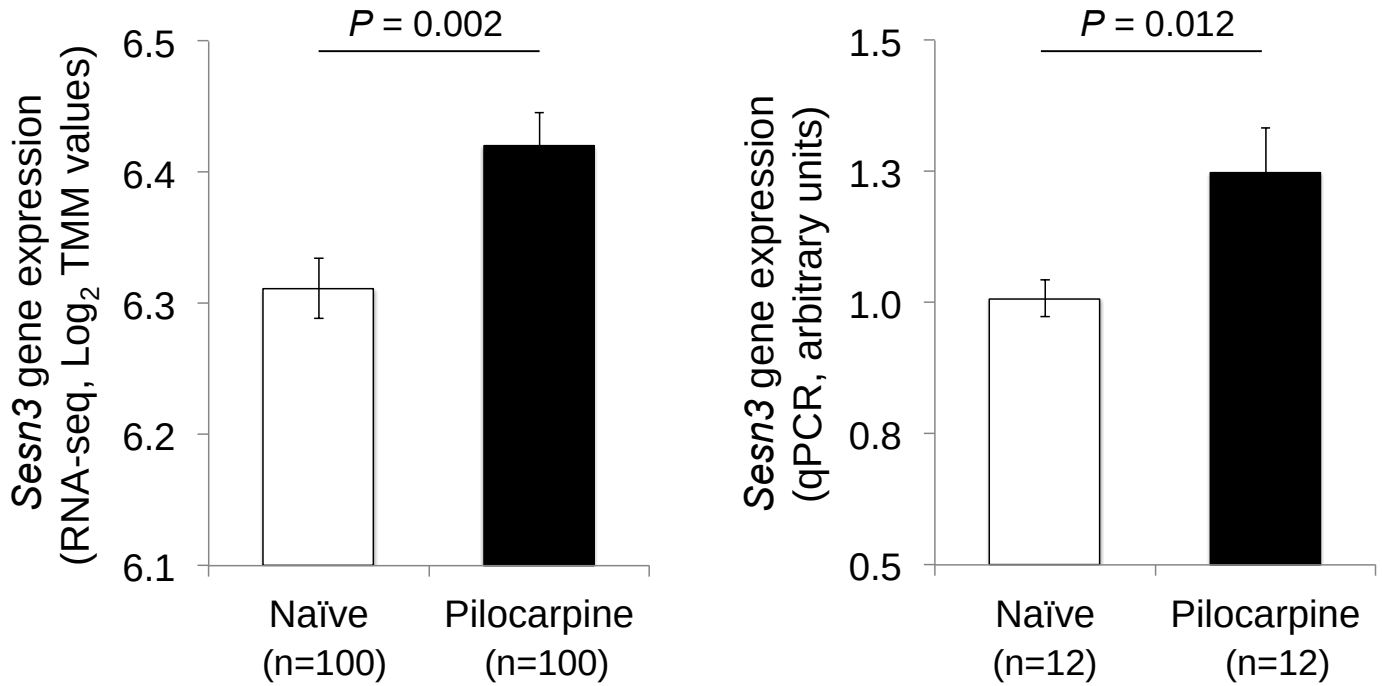

Sesn3 gene expression is increased in the mouse hippocampus after pilocarpine treatment *vs* naïve mice by RNA-Seq (left) and by qPCR (right) analysis. Non-parametric Mann-Whitney test (2-tailed) was used to assess differences between mean *Sesn3* mRNA expression in pilocarpine-treated *vs* naïve mice. TMM, trimmed mean of M-values. In the qPCR analysis *Sesn3* expression levels were normalized to *Gapdh* (endogenous control). All data are reported as mean gene expression ± S.E.M and sample sizes are indicated in the figure.

Supplementary Figure 11: Expression of sesn3 mRNA in the zebrafish larval brain.

In situ hybridization analysis of sesn3 mRNA expression in 3 dpf and 4 dpf zebrafish larvae. Lateral views of larvae (left panels) showing widespread expression of sesn3 in larval brain. Transverse sections through the hindbrain (right panels) reveal extensive expression of sesn3 in brain tissue, which is increased in 4 dpf larvae compared to 3 dpf larvae. dpf, days post fertilization. Probe specificity was tested and validated in independent experiments using *sesn3* antisense and *sesn3* sense (control) probes. Scale bar in left panels = 200 μm; scale bar in right panels = 100 μm.

Supplementary Figure 12: **Microinjection of *sesn3* morpholinos into zebrafish embryos.**

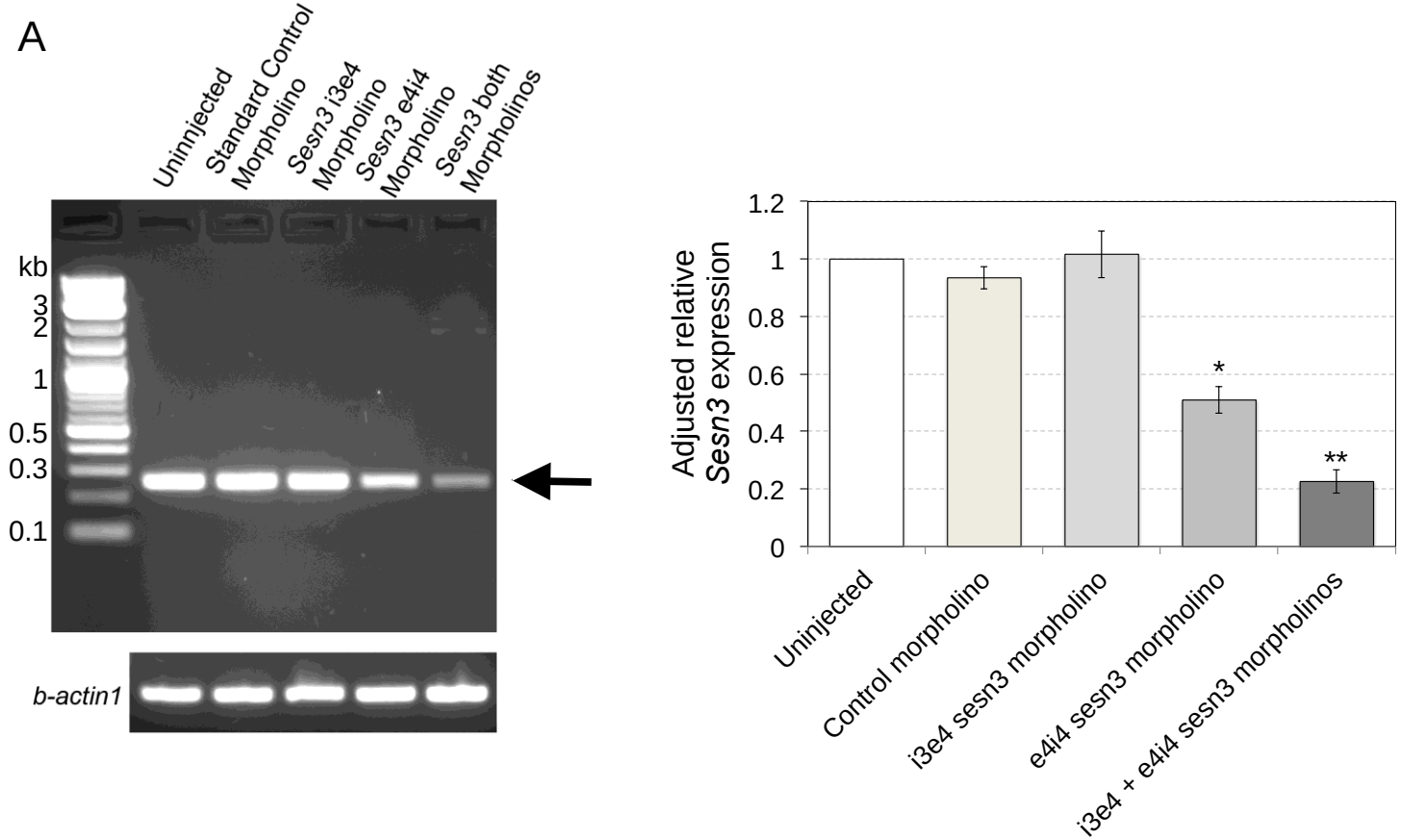

(**A**) Morpholino-mediated knock-down of *sesn3* mRNA levels in zebrafish embryos. RT-PCR analysis of *sesn3* mRNA expression in uninjected embryos and embryos injected with standard control, *sesn3 i3e4*, *sesn3 e4i4*, or *sesn3 i3e4* plus *sesn3e4i4* morpholinos. Injection of both *sesn3 i3e4* and *e4i4* morpholinos reduced the level of processed *sesn3* mRNA (arrowhead) to a much greater extent than did injection of either morpholino alone. The histogram on the right shows that injection of both morpholinos causes an ~80% reduction of *sesn3* mRNA relative to the *sesn3* mRNA level in uninjected embryos (100%). Separate quantitative qPCR data confirmed the significant reduction of *sesn3* mRNA relative to the *sesn3* mRNA level in uninjected embryos. Values were normalized with beta-actin loading controls and are represented as mean ± s.e.m (n=3 in each group). *, $P = 0.001$; **, $P = 2 \times 10^{-5}$ (Mann-Whitney t-test, 2-tailed).

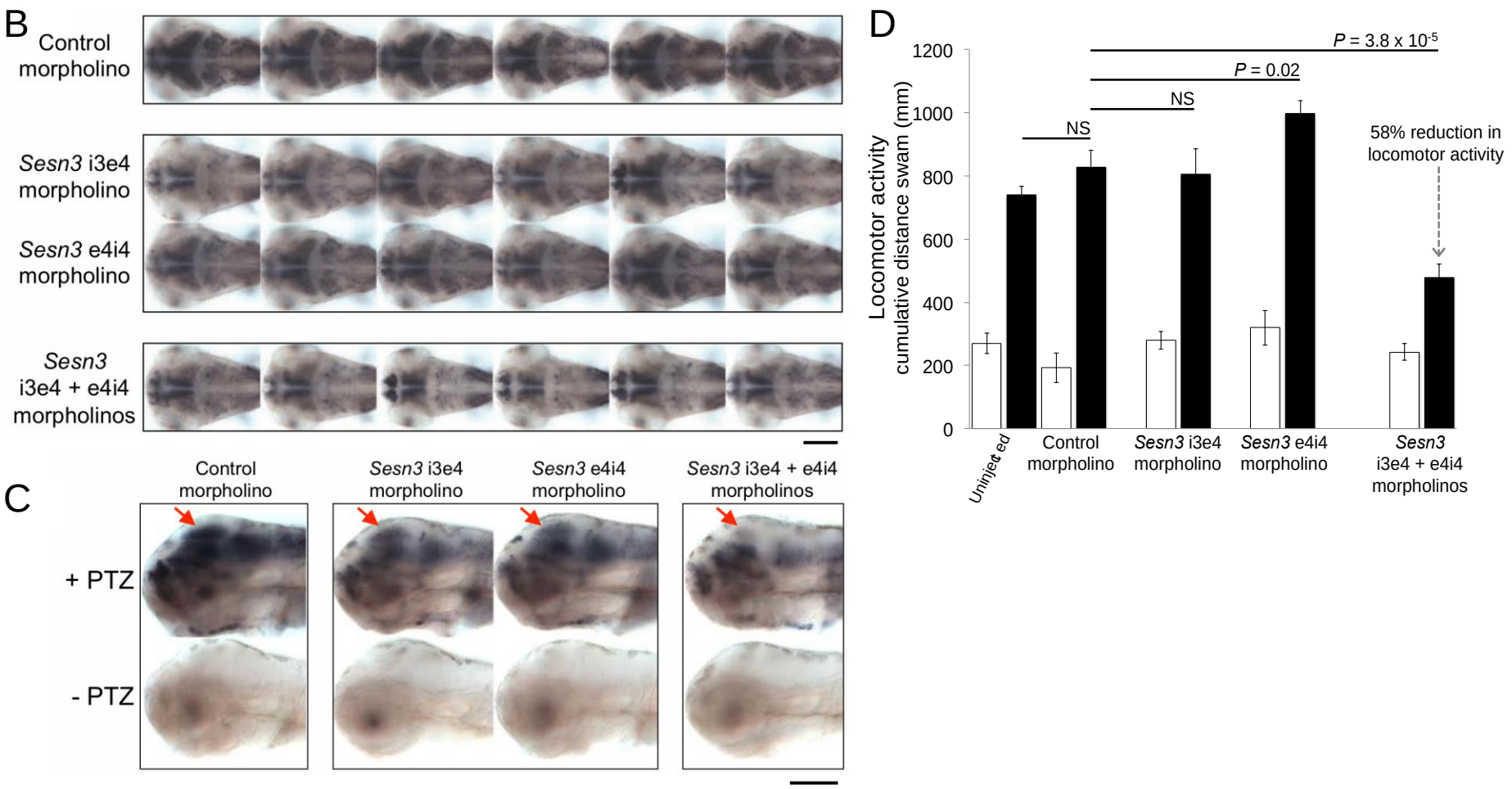

(**B**) Upper row shows PTZ-induced *c-fos* expression in the brain of 6 different 3 dpf sibling larvae microinjected with a control morpholino. Middle two rows show the effect of each morpholino (either i3e4 or e4i4) on PTZ-induced *c-fos* expression in the brain of 6 different sibling larvae. Lower row shows *c-fos* expression in the brain of 6 different larvae microinjected with the combination of the two *sesn3* morpholinos. Combined microinjection of *sesn3 i3e4* and *e4i4* morpholinos inhibited PTZ-induced *cfos* expression more robustly than microinjection of either morpholino individually. Scale bar = 200 μm. (**C**) Upper row: lateral views of representative larvae from panel (**A**), showing effect of *sesn3* morpholinos (i3e4 and e4i4) on PTZ-induced *c-fos* expression. Red arrows

indicate optic tectum, where reduction in *c-fos* expression due to morpholino injection is most pronounced. Lower row shows individuals from the same pools of morpholino-injected embryos that were not treated with PTZ, and consequently no *c-fos* expression is detectable. Scale bar = 200 μm. (**D**) PTZ-induced locomotor activity of larvae injected with the combination of sesn3 morpholinos (i3e4 + e4i4) is much lower than that observed in controls and larvae injected with either *sesn3* morpholino individually. Following PTZ treatment, injection of the combination of two *sesn3* morpholinos yields a 58% reduction in the cumulative distance swam as compared with the control morpholino (P = 3.8 x 10^{-5}). Notably, microinjection of either morpholinos singly showed no significant effect or slightly increased locomotor activity as compared to larvae injected with control morpholino, after PTZ treatment. Black bars, cumulative locomotor activity in zebrafish exposed to 20mM PTZ. White bars, cumulative basal locomotor activity in larvae not treated with PTZ. Data are reported as mean ± s.e.m. NS, not significant (P>0.05).

Supplementary Figure 13: Partial correlations between gene expression profiles in the human hippocampus of TLE patients.

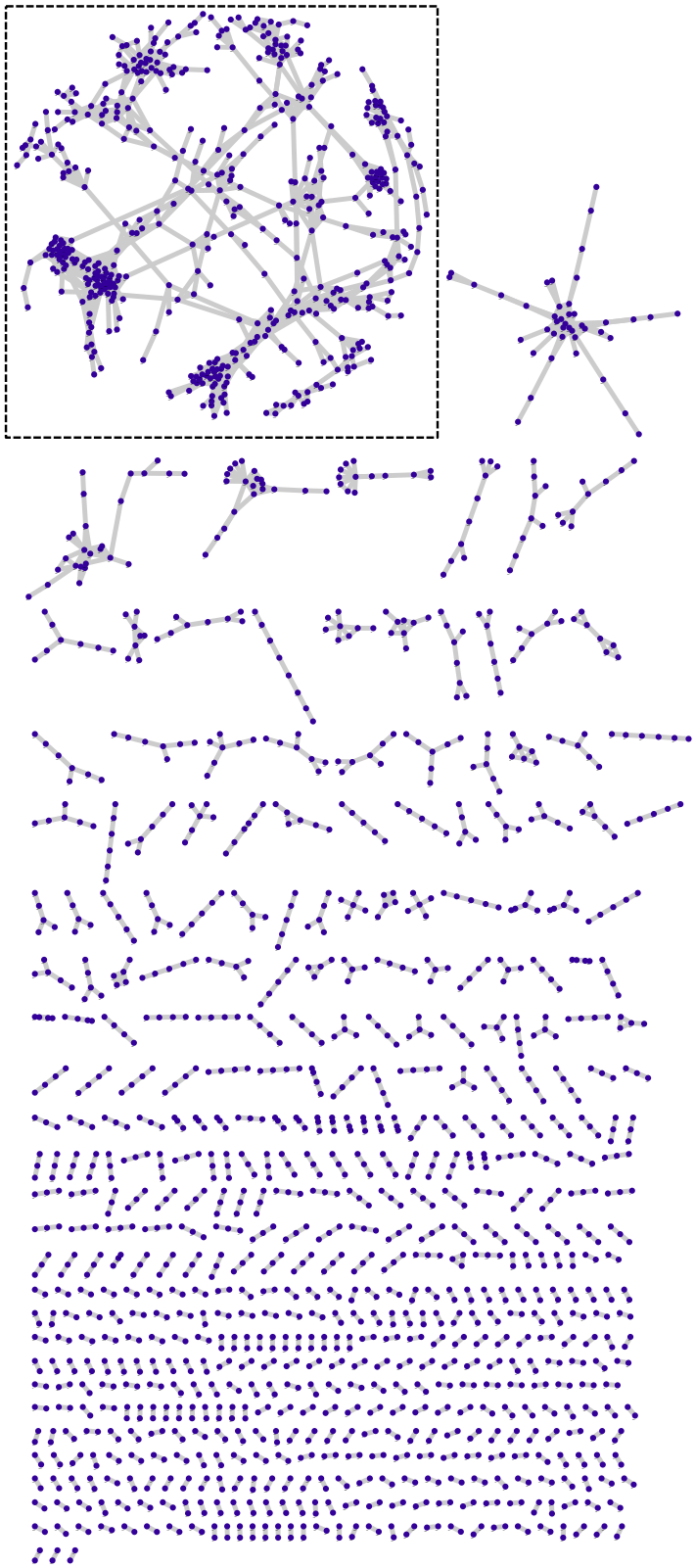

Significant partial correlations identified at 5% False Discovery Rate (FDR). Each node represents an Illumina probe, and each edge connecting any two nodes represents a significant partial correlation between the genes' expression profiles. A total of 2,124 nodes (representing 1,383 annotated genes, reported in Supplementary Data 2) connected by 2,496 edges were identified. The majority of the correlated nodes belong to small components of less than 50 nodes. None of these smaller modules was individually enriched (FDR<5%) for specific GO terms or KEGG pathways.

One large inter-connected component was apparent (indicated by the dotted line square), which was then extracted using clustering algorithms. This component included the top twenty highly inter-connected genes (i.e., hub genes) and included 442 annotated genes (please refer to Fig. 1 and the main text).

The large extracted component ("TLE-network") was enriched for several KEGG pathways including the "Toll-like receptor signaling pathway", the "NOD-like receptor signaling pathway" and the "chemokine signaling pathway" (detailed functional annotation of the TLE-network is reported in Fig. 1b and discussed in the main text).

Supplementary Table 1. Clinical Samples.
Genome-wide expression data were generated from whole human hippocampus samples from 131 patients who had undergone selective amygdalahippocampectomy for mesial temporal epilepsy (mTLE) with hippocampus sclerosis (HS). Clinical data recorded from each patient included: date of birth, sex, handedness, age at epilepsy onset, laterality of TLE (right/left), operation date, age at operation, pre-operative seizure type/s and frequency, antiepilepsy drug (AED) therapy at time of surgery, pathology. Pre-operative seizure frequency was estimated by a retrospective review of the hospital case records for the immediate pre-operative period defined by an absence of change in AED type or dose and expressed as seizures per month. Full clinical and gene expression data were available for 129 out of 131 samples, which were used for the network and genetic analyses. Simple partial seizures were not counted.

Total number of hippocampus samples	131
Number of subjects with HS[1] alone	97 (74%)
Number subjects with dual pathology	34 (26%)
Average age at surgery [range, median]	33 years 4 months [1-64 years, 35 years]
Female	59 (45%)
Male	72 (55%)
Number of subjects with CPS[2] alone	122
Number of subjects with PSG[3]	9
Average number of seizures (CPS + PSG) per month [range, median]	15.1 [150, 5]

[1]HS, hippocampus sclerosis;
[2]CPS, complex partial seizures;
[3]PSG, partial-onset secondary generalized seizures.

Supplementary Table 2. Association of network genes with susceptibility to focal epilepsy.
Ensembl genes were mapped to all SNPs in a 100kb region around the gene transcription start site. Network genes were tested for over-representation in the GWAS data for focal epilepsy (Supplementary Figure 3) using the hypergeometric distribution test. The test significance (enrichment *P*-value) was estimated empirically by 1,000,000 permutations, with the size of the sample drawn equal to that of the set analysed. Enrichment analysis was performed for three SNP sets: intragenic SNPs; SNPs within a 10kb window and SNPs within a 100kb window around the gene transcription start site.

SNP set tested	**Enrichment *P*-value**	**Number of genes with SNP having GWAS *P*-value <0.05**
Intragenic SNPs	2.0×10^{-7}	83
SNPs <10kb window	2.2×10^{-7}	24
SNPs <100kb window	2.1×10^{-7}	42

Supplementary Table 3. Results of the Gene Ontology (GO) enrichment analysis for the genes in Module-1 and Module-2, respectively. The enrichment analysis was carried out using DAVID[2]. Only GO terms showing significant enrichment are reported (false discovery rate (FDR) < 5%).

Module-1

GO Term	Count	%	*P*-value	Fold Enrichment	FDR
Response to wounding	20	29.4	3.40E-14	8.7	<0.01
Inflammatory response	15	22.1	5.70E-12	10.6	<0.01
Response to glucocorticoid stimulus	9	13.2	4.40E-11	26.5	<0.01
Behavior	16	23.5	9.40E-11	7.8	<0.01
Response to organic substance	19	27.9	9.50E-11	6	<0.01
Response to corticosteroid stimulus	9	13.2	9.60E-11	24.3	<0.01
Immune response	18	26.5	4.00E-10	6	<0.01
Response to steroid hormone stimulus	11	16.2	5.50E-10	13.1	<0.01
Response to endogenous stimulus	14	20.6	1.40E-09	7.9	<0.01
Taxis	10	14.7	1.50E-09	14.3	<0.01
Chemotaxis	10	14.7	1.50E-09	14.3	<0.01
Response to hormone stimulus	13	19.1	4.60E-09	8.1	<0.01
Defense response	16	23.5	4.90E-09	6	<0.01
Regulation of cell proliferation	17	25	2.30E-08	5	<0.01
Locomotory behavior	11	16.2	2.30E-08	9.2	<0.01
Negative regulation of cell proliferation	12	17.6	3.90E-08	7.6	<0.01
Regulation of cell cycle	11	16.2	1.60E-07	7.6	<0.01
Apoptosis	14	20.6	2.10E-07	5.3	<0.01
Programmed cell death	14	20.6	2.60E-07	5.3	<0.01
Death	15	22.1	3.20E-07	4.8	<0.01
Cell motion	12	17.6	7.60E-07	5.8	0.01
Response to organic cyclic substance	7	10.3	8.90E-07	13.3	0.02
Response to lipopolysaccharide	6	8.8	9.90E-07	17.9	0.03
Positive regulation of multicellular organismal process	9	13.2	1.00E-06	8.5	0.01
Regulation of smooth muscle cell proliferation	5	7.4	1.60E-06	24.9	0.07
Cell death	14	20.6	1.80E-06	4.5	0.01
Response to molecule of bacterial origin	6	8.8	1.90E-06	16	0.05
Positive regulation of cytokine production	6	8.8	2.50E-06	15.3	0.07

GO Term	Count	%	P-value	Fold Enrichment	FDR
Negative regulation of apoptosis	10	14.7	2.70E-06	6.5	0.03
Negative regulation of programmed cell death	10	14.7	3.00E-06	6.4	0.03
Negative regulation of cell death	10	14.7	3.10E-06	6.4	0.03
Response to mechanical stimulus	5	7.4	4.30E-06	20.5	0.15
Response to extracellular stimulus	8	11.8	4.70E-06	8.3	0.07
Leukocyte migration	5	7.4	4.70E-06	20.1	0.16
Regulation of apoptosis	14	20.6	6.60E-06	4	0.04
Regulation of programmed cell death	14	20.6	7.40E-06	4	0.05
Response to organic nitrogen	5	7.4	7.70E-06	18.2	0.24
Regulation of cell death	14	20.6	7.80E-06	3.9	0.05
Positive regulation of smooth muscle cell proliferation	4	5.9	9.40E-06	29.6	0.50
Positive regulation of cell proliferation	10	14.7	1.10E-05	5.5	0.10
Regeneration	5	7.4	1.20E-05	16.6	0.34
Leukocyte chemotaxis	4	5.9	1.90E-05	24.8	0.84
Response to bacterium	7	10.3	2.00E-05	8.3	0.27
Cell migration	8	11.8	2.40E-05	6.6	0.27
Positive regulation of cell division	4	5.9	2.40E-05	23.5	0.98
Cell chemotaxis	4	5.9	2.40E-05	23.5	0.98
Response to abiotic stimulus	9	13.2	2.80E-05	5.6	0.26
Regulation of viral genome replication	3	4.4	2.80E-05	49.1	2.50
Response to temperature stimulus	5	7.4	3.00E-05	13.8	0.70
Response to oxygen levels	6	8.8	3.30E-05	9.8	0.54
Response to corticosterone stimulus	3	4.4	4.20E-05	43	3.30
Regulation of cell division	4	5.9	5.10E-05	19.5	1.70
Localization of cell	8	11.8	5.20E-05	6	0.52
Cell motility	8	11.8	5.20E-05	6	0.52
Neutrophil chemotaxis	3	4.4	6.10E-05	38.2	4.20
Regulation of response to external stimulus	6	8.8	6.50E-05	8.7	0.94
Negative regulation of multicellular organismal process	6	8.8	7.70E-05	8.4	1.10
Positive regulation of macromolecule biosynthetic process	11	16.2	1.00E-04	3.9	0.66
Female pregnancy	5	7.4	1.10E-04	10.4	2.00
Positive regulation of cell cycle	4	5.9	1.10E-04	16.1	2.90
Regulation of cytokine production	6	8.8	1.30E-04	7.6	1.70
Positive regulation of cellular biosynthetic process	11	16.2	1.60E-04	3.7	0.95

GO Term	Count	%	P-value	Fold Enrichment	FDR
Positive regulation of biosynthetic process	11	16.2	1.80E-04	3.6	1.10
Protein kinase cascade	8	11.8	1.90E-04	5	1.60
Response to vitamin	4	5.9	1.90E-04	13.9	4.50
Positive regulation of protein transport	4	5.9	2.00E-04	13.7	4.60
Anti-apoptosis	6	8.8	2.70E-04	6.7	2.90
Response to hypoxia	5	7.4	2.90E-04	8.6	4.10
Blood vessel morphogenesis	6	8.8	3.00E-04	6.5	3.30
Negative regulation of transport	5	7.4	3.00E-04	8.5	4.20
Response to drug	6	8.8	3.40E-04	6.4	3.60
Regulation of system process	7	10.3	3.70E-04	5.2	3.20
Positive regulation of protein kinase activity	6	8.8	4.10E-04	6.2	4.10
Positive regulation of nitrogen compound metabolic process	10	14.7	4.20E-04	3.6	2.50
Positive regulation of kinase activity	6	8.8	4.90E-04	6	4.80
Protein amino acid phosphorylation	10	14.7	5.60E-04	3.4	3.20
Negative regulation of molecular function	7	10.3	5.90E-04	4.8	4.70

Module-2

GO term	Count	%	P-value	Fold Enrichment	FDR
Collagen fibril organization	4	7.4	1.10E-06	50.4	0.09
Extracellular matrix organization	5	9.3	8.70E-06	17.6	0.24
Blood vessel development	6	11.1	4.80E-05	9	0.66
Vasculature development	6	11.1	5.50E-05	8.7	0.74
Extracellular structure organization	5	9.3	7.60E-05	11.2	1.30
Response to nutrient levels	5	9.3	1.90E-04	9.3	2.60
Response to inorganic substance	5	9.3	2.20E-04	8.9	3.00
Response to extracellular stimulus	5	9.3	3.10E-04	8.3	3.90

Supplementary Table 4. Primer sequences used in the mouse qRT-PCR experiments and *Sesn3* siRNA target sequences.

Primer sequences		
Gene	**Forward sequence**	**Reverse sequence**
IL-1b	GGGCCTCAAAGGAAAGAATC	TACCAGTTGGGGAACTCTGC
IL-1a	CCCGTCCTTAAAGCTGTCTG	AATTGGAATCCAGGGGAAAC
ILRN	TAGCAAATGAGCCACAGACG	ACATGGCAAACAACACAGGA
Nlrp3	ATGCTGCTTCGACATCTCCT	AACCAATGCGAGATCCTGAC
Atf3	TTTTCCGGGAGTTTCATCAG	GGTGTCGTCCATCCTCTGTT
Ccl4	AGCCAGCTGTGGTATTCCTG	GAGGAGGCCTCTCCTGAAGT
Cd69	TGGTGAACTGGAACATTGGA	CTCACAGTCCACAGCGGTAA
Egr2	TTTGATGTGCACTGCTCTCC	TCACACAAGGCACAGAGGAC
Egr3	AGACGTGGAGGCCATGTATC	GGGAAAAGATTGCTGTCCAA
Fos	CTCCCGTGGTCACCTGTACT	TTGCCTTCTCTGACTGCTCA
Fosb	AGAGGTCGAGGCAATTTTCA	GGAGGGAAGGGACAGAACTC
Gadd45B	CACCCTGATCCAGTCGTTCT	TGACAGTTCGTGACCAGGAG
Junb	CCATCAGCTACCTCCCACAT	GCTTTCGCTCCACTTTGATG
Sesn3	GCGAGGAGAAGAACATTTGC	TGTGGTCGTGTCAACATCCT
Tnfa	TATGGCTCAGGGTCCAACTC	CTCCCTTTGCAGAACTCAGG
Hprt	AAGCTTGCTGGTGAAAAGGA	TTGCGCTCATCTTAGGCTTT
Gapdh	GGGTGTGAACCACGAGAAAT	GTCTTCTGGGTGGCAGTGAT

***Sesn3* siRNA target sequences**	
Target sequence 1:	GCAUCAAUCCAGAGAGAGA
Target sequence 2:	GGCUGAAUGGCUUGGAAUA
Target sequence 3:	AGUUCUACAUGCUGCGUAU
Target sequence 4:	AAGCAAAUACGGCGGAUGA

SUPPLEMENTARY METHODS

Pilot study using surgical hippocampus samples

We first assessed the extent of differences in gene expression between hippocampus subfields and between whole hippocampus between individuals using surgical hippocampus samples from five patients with mesial temporal lobe epilepsy (mTLE). For each hippocampus sample, four hippocampus subfields were laser micro-dissected (dentate gyrus, CA1, CA3 and CA4) and genome-wide expression profiles were generated for each subfield using Affymetrix microarray (n=22,215 probe sets) as described before in detail[6]. We found substantially higher inter-individual variability in whole-hippocampus gene expression than between hippocampal subfields (see Supplementary Figure 1), indicating that inter-individual variability in gene expression from whole hippocampus can be used to correlate with variation in phenotype, and informing the use of expression data from whole hippocampus in our subsequent expression analyses.

Clinical material

One hundred and forty seven patients with pharmacoresistant temporal lobe epilepsy (TLE) were studied, who underwent surgical treatment in the Epilepsy Surgery Program at the University of Bonn Medical Center. All patients had undergone a detailed pre-surgical evaluation using a combination of non-invasive and invasive procedures to establish that their seizures originated in the mesial temporal lobe[7]. Surgical removal of the hippocampus was clinically indicated in every case. All procedures were conducted in accordance with the Declaration of Helsinki and approved by the ethics committee of the University of Bonn Medical Center. Informed written consent was obtained from all patients. For the individual patients, the frequency of partial seizures occurring with impairment of consciousness (corresponding to the concept of a complex partial seizure) and partial seizures involving into bilateral tonic, clonic or tonic-clonic components (corresponding to the concept of a secondary generalized seizure) were assessed in the immediate pre-surgical period defined by an absence of change in drug therapy. Subjective sensory or psychic phenomena (simple partial seizures or auras) were not counted. Complex partial and secondary generalized seizures were each counted as

one event, and the combined total expressed as seizures per month. Clinical assessment was by review of the hospital case records from the single centre in the pre-surgical assessment period. Additional clinical variables recorded include: age and sex, handedness, laterality of TLE (determined by standard pre-surgical electro-clinical assessment including high quality structural magnetic resonance imaging), age at manifestation of epilepsy, antiepileptic drug (AED) therapy during the period of seizure frequency assessment (including type and dose for each AED), outcome of surgery and hippocampal pathology. For AED therapy, we grouped patients into one of the following three categories; (A) sodium channel blocker/s alone (B) combination therapy including an SV2A AED (C) combination therapy not including an SV2A AED (overview on clinical data in Supplementary Table 1 and[8]).

Effect of antiepileptic drug therapy, laterality and pathology on gene expression in the hippocampus of temporal lobe epilepsy patients

Genome-wide differential expression analyses were carried out to assess the extent to which each clinical cofactors affect variation in gene expression. No or limited effect of these clinical cofactors was found on gene expression in the hippocampus as detailed below.

Effect of AED therapy: The AED therapies at the time of surgery were classified into three main groups: Category A, patients taking a sodium channel blocker only (n=27), Category B, combination AED therapy that included levetiracetam (n=49) and Category C, combination AED therapy not including levetiracetam (n=52). Differential expression analysis using Significance Analysis of Microarrays (SAM)[1] followed by multiple testing correction did not identify significant differences between the three categories (false discovery rate (FDR) < 5%).

Effect of laterality of temporal lobe epilepsy: Differential expression analysis did not show any significant variation (FDR < 5%) in gene expression due laterality in the study sample.

Effect of pathology: SAM analysis showed a small set of genes that were differentially expressed between the 98 subjects with hippocampal sclerosis as a single pathology and 33 subjects associated

with dual pathology (i.e., hippocampal sclerosis plus an additional adjacent brain lesion)(see Supplementary Table 1). At 5% FDR, 3,151 protein coding genes were identified as differentially expressed. Of these, only 10 genes were also found in the network and significantly associated with seizure frequency (empirical *P*-value <5%).

Sample preparation and microarray analysis in human hippocampus

All 129 patients used in the present study had mesial temporal lobe epilepsy (mTLE) and all tissue samples were from indistinguishable hippocampal tissue portions. Fresh frozen sections were neuropathologically analyzed according to international standards and carefully matched for excellent anatomical preservation by experienced neuropathologists of the Dept. of Neuropathology Bonn. Up to 8 sections of 50.o µm were used for genomic DNA and total RNA isolation. Total RNA was isolated from hippocampal tissue samples using AllPrep DNA/RNA Mini Kit (Qiagen, Hilden) according manufacturer's protocol. Tissue lysate was passed trough an AllPrep RNeasy spin column to selectively isolate RNA. For all cases the RIN-range was from 6,5 to 10. In order to synthesize cDNA from total RNA and in vitro transcription to biotin-labeled cRNA, Illumina TotalPrep-96 RNA Amplification Kit (Life Technologies Corporation, Darmstadt) was used according to the manufacturer's protocol. Briefly, a reverse transcription procedure was applied to synthesize first strand cDNA from 50.o ng total RNA. Second strand synthesis to convert the single-stranded cDNA to double-stranded DNA was carried out. After cDNA purification, *in vitro* transcription was performed for biotin-labeling and following purification of the resulted cRNA. A total amount of 750.o ng cRNA was used for hybridization on Human HT-12 v3 Expression Bead Chips with Illumina Direct Hybridization Assay Kit (Illumina, San Diego, CA). Preparation of cRNA samples and BeadChips was done separately in BeadChip Hyb Chambers and the incubation was carried out overnight to hybridize the labeled cRNA strand to the beads containing respective complementary gene-specific sequences. BeadChips from overnight hybridization were cleaned in several washing steps. To detect the differential signals on the BeadChip, Cy3-Streptavidin was incorporated to bind to the hybridized probes. The Illumina BeadArray Reader was used to scan the excited fluorescent signals of the hybridized single-stranded product on the BeadChips. The data were further analyzed using Illumina's

GenomeStudio Gene Expression Module and were normalized by means of quantile normalization with background subtraction. The microarray probes were annotated using either the Human HT-12 v3 annotation file from Illumina or Ensembl (Human release 72).

Gene co-expression network analysis in the human hippocampus

For each probe, we first removed the effect of "age" and "gender" covariates from the expression data using linear model in R (http://www.r-project.org/). The residuals obtained from the linear regression were used as the input for the network analyses, which was carried out at the level of microarray probes. Gene co-expression networks were inferred using Graphical Gaussian Models (GGMs), which use partial correlations to assess co-expression relationships between any microarray probe pair in the dataset, removing the effect of other probes[9]. To maximize power to detect significant and sizeable partial correlations and co-expression networks, we prioritized probes showing both robust expression (i.e., probes expressed with a detection p-value < 0.05 in at least 20% of the samples) and the highest variation in gene expression (i.e., probes having a coefficient of variation (CV) of gene expression greater than the median CV calculated across all probes in the set). This delineated an informative set of 7,150 probes that were used in the GGM analysis, which was carried out using the package "*GeneNet*"[9,10] in R (http://www.r-project.org/). For each pair of probes, partial correlations were estimated using a shrinkage estimator implemented in "*GeneNet*" package (for details about the shrinkage procedure refer to the original paper[9]). We then used the empirical Bayes local FDR statistic[11] to extract significant edges from the set of partial correlations (Supplementary Figure 13), which delineated a set of 2,124 inter-connected nodes (Supplementary Data 2).

Network extraction: We employed the Heinz algorithm[12], implemented in the R package *BioNet*[13], to extract the largest connected component of 511 nodes (i.e., probes) from the set of partial correlations encompassing 2,124 nodes (Supplementary Data 2), which were detected at FDR 5%. This defined a co-expression network of 511 nodes, representing 442 annotated unique genes (Supplementary Data 1), which we called TLE-hippocampus derived transcriptional network (TLE-network).

Identification of transcriptional modules: The *ClusterViz* package on the Cytoscape platform[14] was used to investigate and extract clusters within the large connected component of 511 nodes. This is based on the fast agglomerative algorithm based on edge clustering coefficients (FAG-EC) developed by[15], which is a modification of the k-means algorithm, was used to extract discrete modules from the large connected component of 511 nodes. Briefly, an undirected simple graph *G* is created from the list of nodes and edges in the large component, and the clustering coefficients ($C_{i,j}$) of all edges in the graph are calculated according to

$$C_{i,j} = \frac{|N_i \bigcap N_j| + 1}{\min(k_i, k_j)} \qquad \text{Equation (1)}$$

where k_i and k_j are the degrees of node *i* and node *j*. The edges are sorted in decreasing order of edge clustering coefficient. The higher the clustering coefficient of an edge, the more likely that it is an edge to be found inside the same module. All the nodes in graph *G* are initialized as singleton sub-graphs, which are mergeable. Edges are gradually added to clusters by working down the ordered list of edges. This procedure yielded two large modules comprising 80 nodes (representing 69 unique annotated genes) with 584 edges (Module-1) and 60 nodes (representing 54 unique annotated genes) with 247 edges (Module-2), respectively.

Mapping the genetic control of gene co-expression networks

Here we illustrate the strategy we used to map the genetic control points of the transcriptional modules in the TLE patient cohort. After preprocessing of the genotype data, we performed the following steps: *i*) Principal Components Bayesian GWA study (PCBGWAs) and *ii*) refinement of genetic mapping results provided by PCBGWAs.

Data preprocessing: imputation of missing values, Minor Allele Frequency (MAF) thresholding and tagging: Genotype data was available for 122 TLE samples. Missing values in the genotype data for each of the 22 autosomal chromosomes were imputed using FastPhase[16], allowing 20 random starts of the EM algorithm (-T20), 100 iterations of the EM algorithm for each random start (-C100), no haplotype estimation (-H-4), without the determination of the number of clusters (-K1). We removed

SNPs with Minor Allele Frequency (MAF) < 0.05 and performed tagging at D′ > 0.80 level[17]. The original data set consisting of 527,684 SNPs was reduced to 478,290 SNPs after MAF thresholding (19% reduction) and further shrunk to 346,408 SNP after tagging (34% reduction). This set of SNPs was used for all following analyses.

Step 1: Principal Components Bayesian GWA study (PCBGWAs)

We performed Principal Component (PC) analysis[18] on Module-1 (n=122 and q=80) and Module-2 (n=122 and q=60) expression separately. The first three PCs (each explaining a proportion of variance > 5%) accounted in total for 76.83% and 51.55% of the variability of Module-1 and Module-2, respectively (Supplementary Figure 6) and were used for the Bayesian GWA study.

We used PC-based multivariate regression approaches[19] to prioritize genomic regions associated with Modules' expression. For each module, the first three PCs were associated to the set of predictors (~350K SNPs) using ESS++ (Evolutionary Stochastic Search)[20,21]. Given the relatively small number of subjects (n=122), in order to detect important signals we imposed very strong sparsity with $E(p_\gamma)$ = 2 and $V(p_\gamma)$ = 2 (i.e., the *a priori* expected model size (expected number of true genetic associations) and variance of the model size), meaning the prior model size is likely to range from 0 to 6. In this set-up, given the level of sparsity and the number of predictors (p=346,408), the average prior probability π that a SNP is truly associated with the phenotype is 5.77×10^{-6}. ESS++, the Bayesian variable selection algorithm, was run for 110,000 sweeps, with 10,000 sweeps as burn-in, with three chains run in parallel and a hyper-prior on the selection coefficient τ. Diagnostic tests for convergence were performed similarly to[22]. Output from the algorithm enabled us to calculate the Best Model visited (which defines the best set of predictors visited, i.e. SNPs) as well as the Marginal Posterior Probability of Inclusion (MPPI) and the associated (local) FDR for each SNP[23]. Following [24], for each predictor (SNP), we derived the Bayes Factor (BF) as the ratio between the Posterior Odds and the Prior Odds. Detailed discussion and the benefits of reporting BF over the more traditional critical level (P-value) of a test of association can be found in[25]. Since in our set-up π is very small, the BF has to be

large ($\log_{10}$(BF)>6) to provide strong evidence for phenotype-SNP association (with MPPI close to 1 and (local) FDR<0.05).

Step 2: Refinement of genetic mapping results provided by PCBGWAs

For the locus on chromosome 11q21 detected by PCBGWAs for Module-1, we refined the association by defining a 1Mbp region centered on the significant SNP. We then linked all genes of the Module to all SNPs in the selected region using HESS[24], the extension of ESS++[21] where a large number of traits (i.e., Module-1 genes' expression) are jointly considered. Sparsity was imposed setting $E(p_\gamma) = 2$ and $V(p_\gamma) = 2$ for each gene with the prior probability π that a SNP at the locus is truly associated equal to 0.0112 for Module-1. The algorithm was run for 110,000 sweeps, with 10,000 sweeps as burn-in, with three chains run in parallel. Convergence diagnostics of the Monte Carlo Markov Chain output showed no evidence of irregular behavior. The Best Model Visited is the most supported multivariate model ranked according to the Model Posterior Probability. For each multivariate model (i.e., any combination gene(s)-SNP(s)) visited during the Markov Chain Monte Carlo, the log-Posterior (log marginal likelihood × log prior on the model space) is available and, for each unique model visited, the Model Posterior Probability is equal to the renormalized log-Posterior probability. Finally the proportion of genes associated with each SNP is defined as the average number of genes that are predicted in the Best Models Visited by each SNP. This measure helps prioritizing SNPs that influence multiple genes at the same time and allows the discovery of so-called regulatory hot-spots, i.e., genetic loci that are associated with a large number of gene expression traits[24].

Genetic association of TLE-network genes with epilepsy susceptibility

To test whether co-expression networks are likely to be causal, we tested whether network genes are enriched for SNP variants genetically associated to epilepsy; since genotypes do not vary with disease status, genetic association of a network to disease susceptibility provides independent evidence for a causal relationship with the disease.

Genome-wide association study (GWAS) of susceptibility to focal epilepsy: To test whether networks show enrichment for epilepsy genetic association signals we undertook an epilepsy GWAS comprising 1,429 patients with focal epilepsy and 7,358 healthy controls. Three epilepsy cohorts of "UK, Swiss or Finnish ancestry" and matched healthy controls were combined via meta-analysis.

Patients: The diagnosis of focal epilepsy was made and/or reviewed by a consultant neurologist according to the International League Against Epilepsy (ILAE) definition of focal epilepsy[26]. All causes of focal epilepsy (genetic, structural and unknown) according to the ILAE Revised Terminology and Concepts for Organisation of Seizures and Epilepsies[27] were included except patients with a progressive brain lesion who were excluded. The 1,429 cases with focal epilepsy available post-filtering (see below) were derived as follows: (a) 806 UK Ancestry cases; (b) 213 Swiss Ancestry cases provided by GSK; (c) 410 Finnish Ancestry cases also provided by GSK. Of the 1,429 patients, 1,013 (71%) had a clinical diagnosis of temporal lobe epilepsy (TLE).

Controls: Post filtering (see below), the 7,358 healthy controls were divided as follows: (a) 5,184 UK controls from the Wellcome Trust Case Control Consortium Phase 2 (WTCCC2), consisting of the 58 Birth Cohort (58 BC; 2,692 controls) and the National Blood Service (NBS; 2,492 controls); (b) 232 Swiss controls provided by GSK; (c) 1,942 Finnish Controls from either the Helsinki Birth Cohort (HBC; 1,671 controls) or GSK (271 controls).

Genotyping, Quality Control and Population Stratification: UK cases were genotyped on Illumina 660-Quad; WT controls were genotyped on Illumina 1.2M. Samples provided by GSK were genotyped on Illumina 610-Quad, HBC samples were genotyped on 660-Quad.

Identification of Close Relatives and Population Structure: For each ancestry band, we first estimated pairwise identity by descent (IBD) by calculating identity by state across a subset of roughly 50,000 of the highest quality SNPs, pruned to ensure approximate linkage disequilibrium. These pairwise IBD values enabled us to remove one of each pair of very close relatives (IBD>0.25) and identify population outliers. For the association analyses, we included covariates representative of population structure across the ancestry band as a whole (e.g. all UK ancestry samples) as well as covariates

specific to a particular set of samples (e.g. just 58 BC controls). We derived these covariates using the top eigenvectors calculated from (a subset of) the IBD estimate matrix. We determined the number of significant axes to include using the Tracy-Widom test implemented in EIGENSTRAT software[28].

Association Analysis: For the association testing across each ancestry band, we retained autosomal SNPs which satisfied the following criteria: MAF > 0.05, Call Rate (CR) > 0.99, p-value from test for Hardy-Weinberg equilibrium (HWE) > 0.0001; additionally SNPs with 0.01 < MAF < 0.05 were retained if CR > 0.995 and HWE > 0.01. We utilized the logistic regression function implemented in PLINK[29]. This fits a linear model to the log odds for susceptibility to focal epilepsy, which is made up of an intercept term, contributions from sex and from the population covariates and for the SNP in question. From the three GWASs, we had p-values for 512,450 SNPs (UK Study) 488,214 SNPs (Swiss Study) and 498,721 SNPs (Finnish Study). This meant that for 487,682/11,571/13,197 SNPs we had 3/2/1 p-values. Association p-values were combined using PLINK's meta-analysis function, which invokes a standard inverse variance weighting[29]. We discovered no single SNP with a genome-wide significant association with susceptibility; all p-values were greater than 10^{-7} (see Supplementary Figure 3), consistent with the hypothesis that focal epilepsy is a highly polygenic trait with no common variants with strong effect sizes[30].

Enrichment analysis of network genes with epilepsy: To examine whether genes in the network were associated with susceptibility to focal epilepsy we first compared the genomic locations of each SNP genotyped in the focal epilepsy GWAS with the Ensembl gene annotations using the GRCh37.p5 build of the Ensembl database (www.ensembl.org). We then divided all SNPs into three major categories: (A) SNPs within any Ensembl gene in the network; (B) SNPs within 10kb region around any Ensembl gene in the network (excluding any in A); (C) SNPs within 100kb region around any Ensembl gene in the network (excluding any in A or B). Each gene was then assigned a GWAS significance value consisting of the lowest P-value of all SNPs mapped to it. We tested whether SNPs close to (<100kb from) any network genes were significantly more likely to associate with epilepsy in GWASs than SNPs close to genes not in the network. We used the hypergeometric distribution test to determine the degree of overrepresentation of significant genetic associations (i.e., GWAS *P*-value < 0.05) within

the network gene set. For each SNP category the null distribution of the hypergeometric test was generated by 1,000,000 randomly selected gene sets, where the size of the sample drawn was equal to that of the set analyzed[31]. This yielded the empirical enrichment *P*-values for the network genes within each SNP category, which are reported in Supplementary Table 2 and show that the distance between the SNPs and the network genes did not affect the reported enrichment results for the network.

RNA-sequencing analysis in the mouse hippocampus

Mouse pilocarpine model: A single injection of pilocarpine was used to trigger status epilepticus (SE) in male NMRI mice (Charles River, France) 28–32 g at the beginning of the study. As previously described[32], animals were injected intraperitoneally (i.p.) with 1 mg/kg of Nmethylscopolamine bromide 30 min prior to pilocarpine treatment (300 mg/kg; i.p.). Within 10 to 45 min after pilocarpine treatment, animals displayed generalized clonic-tonic seizures that progressed to continuous convulsive activity, i.e. status epilepticus. The SE lasted 3 h and was interrupted by i.p. injection of diazepam (10 mg/kg) to limit the extent of brain damage. The mice surviving SE typically show spontaneous recurrent seizures within few days and continue to display them for several weeks[32]. In the present study all mice were continuously video monitored for a period of 2 weeks starting the recordings 4 weeks after pilocarpine-indeed SE to document the presence of spontaneous recurrent seizures. The mice were then scarified 6 weeks after SE induction to collect brain samples.

RNA-Seq analysis: We carried out high-throughput sequencing of mRNA (RNA-Seq) in whole hippocampus from 100 epileptic (pilocarpine model where spontaneous recurrent seizures were document by video monitoring of each individual animal)[32] and 100 control naïve mice. Total RNA was isolated from 200 mouse hippocampi and cDNA and sample preparation for RNA sequencing was done according to the protocols recommended by the manufacturers (TruSeq RNA kit, Illumina). Samples were sequenced on an Illumina HiSeq 2000 sequencer as paired-end 75-nucleotide reads according to the protocol recommended by the vendor. Raw reads were mapped to the reference mouse genome (mm10) using TopHat version 2.0.8[33]. Read counts per gene were calculated for each sample using HTseq version 0.5.3. Read counts per gene were further normalised across all samples

using the "trimmed mean of M-value" (TMM) approach as discussed in[34]. Differential expression analysis was performed using the Bioconductor R package *edgeR*[34] version 3.2.4, and a threshold of 5% FDR was used to identify significant gene expression changes.

Cell culture and *in vitro* experiments

Bone-marrow-derived macrophages (BMDMs) from C57BL/6J mice were cultured in L929 conditioned media as previously described[35]. Briefly femurs and tibias from each mouse were flushed out in HBSS (Life Technologies) with the use of a syringe. Total bone marrow-derived cells were plated in 6-well plates (Nunc) and cultured for 5 days in DMEM (Life Technologies) that contained 25 mM HEPES (Sigma), 25% L929 conditioned medium, 25% FBS (Biosera), penicillin (100 U/ml; Life Technologies), streptomycin (100 µg/ml; Life Technologies), and l-glutamine (2 mM; Life Technologies). Following 5 days of differentiation, these cells were characterized as macrophages by CD68 staining.

Murine microglial cell line (BV2) was kindly provided by Dr Joseph Bertrand (Karolinska institute, Sweden). BV2 cells were cultured and maintained in DMEM (Life Technologies) media and supplemented with 10% FBS (Biosera), 2 mM L-glutamine, penicillin (100 U/ml, Life Technologies) and streptomycin (100 mg/ml, Life Technologies).

Hippocampal neurons were derived from embryonic mice[36]. Embryonic day 19 mice were harvested by cesarean section after culling the pregnant dams by cervical dislocation (strain GFPm-high, bred in our facility). The animal protocol was approved by the local ethics committee and performed under UK Home Office License. Brains were removed from the embryos and hippocampi were isolated from each brain hemisphere after removing meninges. Hippocampal tissue was then dissociated by 2.5% (wt/vol) trypsin digestion and trituration with a Pasteur pipette and a fine 1000 µl bore pipette. Low-density cultures (5×10^4 cells/ml) were plated onto 18 mm glass cover-slips introduced into 12-well (3 cm^2) culture dishes. Tissue culture dishes were coated with (0.01mg/ml) poly-L-lysine. The cells were plated in Neurobasal medium (Life Technologies) supplemented with B27 (Life Technologies), 200mM glutamine (Life Technologies), 14.3M β-mercaptoethanol and streptomycin/amphotericin B

(Life Technologies). Hippocampal tissue preparations were incubated in the cell culture incubator at 37°C, 5% CO_2 . Two days after plating, the medium was top up with 30% of the initial volume and after 3 more days 50% of the medium was changed. Subsequently every 4-5 days 50% of the medium was replaced. Hippocampal cultures were maintained for up to 10 days *in vitro*.

SESN3 silencing and assessment of Module-1 gene expression by qRT-PCR: siRNA knockdown experiments were performed in BMDMs or BV2 microglia cell lines by using a mouse Sesn3 ON-TARGETplus SMARTpool siRNA (100nM, ThermoFisher Scientific) and Dharmafect 1 (1:50, ThermoFisher Scientific) a transfection reagent, according to manufacturer's recommendations. Briefly, cells cultured in 6-well plates were incubated in serum and antibiotic free DMEM for 10 h and transfected for 48 h with SESN3 siRNA, which consists of a pool of four unique siRNA molecules against mouse SESN3, using Dharmafect 1 in OPTIMEM medium (Life Technologies). Control cells were transfected in the same conditions with non-targeting scrambled siRNA (100 nM). For lipopolysaccharide (LPS) stimulation experiments, the transfected BMDM cells were washed twice in DMEM and stimulated with LPS (Sigma, 100 ng/ml) for an hour. Cells (basal or LPS-stimulated) were then harvested in TriZOL (Life Technologies) and total RNA was extracted according to manufacturer's instructions. Real-time one step RT-PCR for Module-1 genes was performed on an ABI 7500 Sequence Detection System (Applied Biosystems, Warrington, UK) using SYBR Green (Stratagene, Cambridge, UK) with 100 ng of total RNA and gene-specific primer sets. Results were then exported to 7500 Fast system SDS software (ABS), and Ct values were determined for all of the genes analysed.

Lentivirus production and assessment of Module-1 gene expression by qRT-PCR: A third generation Lentiviral Vectors (LV) was used to transduce murine primary hippocampal neuronal culture. The LV was prepared by Calcium Phosphate transfection. Briefly, co-transfection of packaging plasmids (pMDLg/pRRE, 12.5 µg, pMD2.VSV-G, 6.25 µg, pRSV-REV, 7 µg) and transfer plasmid (pLCMV-Sesn3-1-Flag, 32 µg) was made in Hek 293T cells. Media was replaced at 18 hours and the harvesting was performed at 36 and 72 hours. The purification was obtained by over-night centrifugation at 4°C and 4,000 rpm. The LV transduction was performed by replacing the media with 33 µl of vector

($4.98*10^{\wedge 7}$ IU/ml) and, to improve the vector penetration 8 μg/ml of polybrene were supplemented to the cells. Three days after the LV transduction the RNA was extracted and the cDNA was synthetized. Real-time one step RT-PCR for Module-1 genes was performed as described above. The relative expression levels normalized to *Beta-actin* or *Gapdh* gene expression (as indicated) were then determined by using the $2^{-\Delta\Delta Ct}$ method.

Zebrafish studies

Microinjection of morpholino antisense oligonucleotides: To study the function of sestrin3 in response to Pentylenetetrazole-induced (PTZ-induced) seizures, two different morpholinos (MOs) were designed to block the normal splicing of the zebrafish *sesn3* primary transcript. Sesn3 i3e4MO targets the splice acceptor site between intron3 and exon 4 of the gene (5'-TGCAGCCTGGAAGACATGGAAAAAA -3') whereas Sesn3 e4i4MO targets the splice donor site between exon 4 and intron 4 (5'-GACTCCAACTAATGGGTTTACTTGT-3'). We assessed the morpholinos efficacy and found that PTZ-induced locomotor activity of larvae injected with the combination of *sesn3* morpholinos (i3e4MO + e4i4MO) was much lower than that of controls and larvae injected with either *sesn3* morpholino individually (Supplementary Figure 12). Sesn3 i3e4MO and Sesn3 e4i4MO were co-injected into AB wildtype zebrafish embryos at the one- or two-cell stage, at a concentration of 0.05mM of each morpholino (total MO concentration 0.1mM) in water. Sesn3 i3e4 + Sesn3 e4i4 MO solution was microinjected in a final volume of approximately 2nl. The standard control morpholino (Gene Tools) was microinjected at a concentration of 0.1mM into one- or two-cell stage AB zebrafish embryos, in a volume of 2nl per embryo. Standard Control Morpholino sequence: 5'-CCTCTTACCTCAGTTACAATTTATA- 3' (Gene Tools). Embryos that were to be analysed by whole mount in situ hybridisation were first treated with 1-phenyl-2 thiourea (PTU) at 23 hours post-fertilization (hpf) to inhibit melanogenesis. At 3 days post-fertilisation (dpf), larvae were treated for one hour with 20mM PTZ or left untreated, and all larvae were then fixed with paraformaldehyde immediately after the treatment period.

RNA in situ hybridisation: A *c-fos* digoxigenin-labelled probe was prepared as recommended by the manufacturer of the in situ hybridisation reagents (Roche). Whole-mount in situ hybridisation was performed using standard procedures; details of the probe used are available on request (Vincent T. Cunliffe, MRC Centre for Developmental and Biomedical Genetics, Department of Biomedical Science, University of Sheffield, UK).

qPCR analysis of c-fos and Module-1 genes: Between 15 and 20 *sesn3* morphant larvae and control larvae were decapitated at 3dpf after 1hr of 20mM PTZ treatment and only the heads were processed for RNA extraction. The heads were treated with 200µl RNAlater (Ambion) and stored at 4°C. The RNA later was discarded and RNA was extracted using 1ml of TRIzol (Invitrogen). The RNA was then treated with 1µl DNase I (Invitrogen) and after a 30 minute incubation at 37°C, the RNA was precipitated with sodium acetate and ethanol. cDNA was synthesized using SuperScript® II First-Strand Synthesis System for RT-PCR kit (Invitrogen). The qPCR reactions were carried out using SYBR Green (Sigma) and 10ng of cDNA final concentration. The reactions were prepared in Hard-Shell® Low-Profile Thin-Wall 96-Well Skirted PCR Plates (BioRad) and the PCR machine used for the analyses was BioRad CFX96 Touch™ Real-Time PCR Detection System. The efficiency of the primers was assayed at 300ng concentration. The relative expression levels normalized to the housekeeping gene *beta-actin* gene expression were then determined by using the $2^{-\Delta\Delta Ct}$ method.

qPCR analysis of Module-1 genes after injection of synthetic sesn3 mRNA in zebrafish embryos: In vitro-synthesized *sesn3* RNA was injected into 1 cell-stage zebrafish embryos (~ 1ng *sesn3* RNA per embryo). At 28hpf, *sesn3* RNA-injected and control uninjected embryos were collected and frozen at -80^0 C. Total RNA was extracted using TRizol (Invitrogen) and isopropanol. The extracted RNA was cleaned up using the RNAeasy mini kit (QIAGEN) before first stand cDNA synthesis was performed using Superscript II Kit (Invitrogen). For the qPCR analyses the reactions were prepared in Hard-Shell® Low-Profile Thin-Wall 96-Well Skirted PCR Plates (Biorad). Each qPCR reaction contained 5µl Sybr green (Sigma), 0.6 µl 5µM forward primer (300ng final concentration), 0.6 µl 5µM reverse primer (300ng final concentration), 1 µl 1:10 cDNA dilution (10ng cDNA final concentration), and 2.8 µl RNase free water. The PCR machine used for the analyses was BioRad CFX96 Touch™ Real-Time

PCR Detection System. The efficiency of the primers was assayed at 300ng concentration. The relative expression levels normalized to the housekeeping gene *beta-actin* were then determined by using the $2^{-\Delta\Delta Ct}$ method.

Primers sequences used for the PCR: Atf3 forward primer 5'-GAGACCCACCGAACTACCTG, reverse primer 5'-TGCTGCTGCAATTTGTTTC; *beta-actin1* forward primer 5'-CAACAACCTGCTGGGCAAA, reverse primer 5'-GCGTCGATGTCGAAGGTCA (Keegan et al., 2002); *cfos* forward primer 5'-TCGACGTGAACTCACCGATA, reverse primer 5'-CTTGCAGATGGGTTTGTGTG; *egr2b* forward primer 5'-CTGCCAGCCTCTGTGACTAT, reverse primer 5'-GCTTCTCCGTGCTCATATCC; *fosB* forward primer 5'-CCAGTGCGTCAGTCTCGAAG, reverse primer 5'-CGGCAGCCAGTTTATTTCTC; *gapdh* forward primer 5'-GTGGAGTCTACTGGTGTCTT, reverse primer 5'-GTGCAGGAGGCATTGCTTAC.

Analysis of zebrafish locomotor activity using the Viewpoint Zebrabox system: The distance moved by larvae over a 1 hour period of PTZ treatment was recorded using the Zebrabox system (Viewpoint, France). AB larvae aged 3 dpf were transferred to a 48-well microlitre plate, one larva per well containing 500ul (for un-treated larvae) or 450ul (for PTZ-treated larvae) of E3 medium. Then 50ul of 200mM PTZ were added into the wells containing 450ul of E3 media to achieve a final concentration of 20mM PTZ. The locomotor behaviour of the larvae was then recorded for 1 hour using the Zebrabox equipment. The recording started immediately after PTZ was added and the Viewpoint software was set to integrate the data for the distance moved every 10 minutes. Locomotor activity of larvae was recorded with the Zebrabox using a light cycle of 2 minutes: 100% light; 2 minutes: 0% light.

Rescue experiments: To investigate if the phenotype observed in *sesn3* morphant larvae was caused by the decreased expression of *sestrin3,* synthetic *sesn3* messenger RNA was co-injected along with *sesn3* morpholinos into zebrafish embryos to determine whether the morphant phenotype could be rescued. A full-length zebrafish *sestrin3* cDNA clone (IMAGE:2601412) was subcloned into the pCS2+ expression vector to create pCS2+.sestrin3. A linearized template of pCS2+.sestrin3 was used

to synthesize *sesn3* RNA using the mMessage mMachine Kit (Ambion). The synthetic *sesn3* RNA was injected into one-cell stage AB wild type zebrafish embryos alone (2nl of 0.3ng/nl sesn3 mRNA) or in combination with *sesn3* morpholinos (2nl of 0.3ng/nl sesn3 mRNA + 0.05mM sesn3 i3e4 MO + 0.05mM sesn3 e4i4 MO). In addition, some embryos were injected with *sesn3* morpholinos alone (2nl of 0.05mM sesn3 i3e4 MO + 0.05mM sesn3 e4i4 MO). The locomotor activity in response to PTZ exposure was analyzed using the Viewpoint zebrabox, as described above.

Immunohistochemistry analysis in human hippocampus from TLE patients

For immunohistochemistry, human hippocampal sections obtained from paraffin blocks were deparaffinized in xylene and rehydrated in a graded alcohol series. After a short step washing in phosphate-buffered saline (PBS), the slides were microwaved in citric acid buffer (10mM, pH 6.0) for 10 min and then washed in PBS. All washing steps were carried out for 2 x 5 min in PBS at room temperature (RT). Slides were blocked for 2 h at 37°C in PBS-blocking buffer (10% fetal calf serum (FCS) and 1% normal goat serum in PBS) to inhibit non-specific antibody binding. Antibodies targeted against polyclonal anti-rabbit antibody SESN3 (1:300; Novus Biologicals, Cambridge), neuronal nuclear protein (NeuN) antibody (1:500; Millipore, Billerica, MA USA) and monoclonal anti-mouse antibody HLA-DR (1:1200; Dako, Hamburg, Germany) were incubated over night at 4°C in PBS including 10% FCS. After washing, both secondary antibodies anti-rabbit Cy3 (1:400; Jackson Research, New Market UK) and anti-mouse FITC (1:400; Jackson Research, New Market UK) were applied, diluted in PBS including 10% FCS for 2h in the dark. After washing, respective slides were covered with VectaShield HardSet Mounting Medium for Fluorescence (Vector Laboratories, Burlingame, CA). Sections were then analyzed with the Axio Observer.A1 microscope (Carl Zeiss, Göttingen, Germany) with HXP 120 fluorescence light system.

Immunohistochemical staining: Human hippocampal paraffin slices were stained with antibodies against SESN3 (1:300; Novus Biologicals, Cambridge UK; NBP1-82717) and MAP2 (1:200; Millipore, Billerica, MA USA; MAB3418).

Quantification of cell fluorescence: Z-stacks of confocal images were generated to obtain maximum

intensity projections. Quantification of cell fluorescence intensity of SESN3 expressing cells in the conserved CA2 region of the hippocampus in both TLE patients samples (n = 7) and autopsy samples without known neurological disorders (n = 8) was carried out using ImageJ software by calculating: total cell fluorescence = integrated density – (area of selected cell x mean fluorescence of background readings). Average background was calculated based on three random regions in the vicinity of the cell count region per section. For each section a region of 167,772 px^2 ≈ 40,000µm^2 was selected and the cellular elements were counted, i.e., corresponding to approximately 20 cellular elements per section. All images were independently and blindly quantified.

REFERENCES

1 Tusher, V. G., Tibshirani, R. & Chu, G. Significance analysis of microarrays applied to the ionizing radiation response. *Proc Natl Acad Sci U S A* 98, 5116-5121 (2001).

2 Huang, D.W., Sherman, B.T. & Lempicki, R.A.. Systematic and integrative analysis of large gene lists using DAVID Bioinformatics Resources. *Nature Protoc*. 4, 44-57 (2009).

3 Rossin, E. J. *et al*. Proteins encoded in genomic regions associated with immune-mediated disease physically interact and suggest underlying biology. *PLoS Genetics* 7, e1001273, doi:10.1371/journal.pgen.1001273 (2011).

4 Li, J.Z., Bunney, B.G., Meng, F., Hagenauer, M.H. *et al*. Circadian patterns of gene expression in the human brain and disruption in major depressive disorder. *Proc Natl Acad Sci U S A* 110(24), 9950-5 (2013).

5 Ravasi, T., Suzuki, H., Cannistraci, C.V., *et al. Cell* 140, 744-753, doi: 10.1016/j.cell.2010.01.044 (2010).

6 Becker, A. J. *et al.* Correlated stage- and subfield-associated hippocampal gene expression patterns in experimental and human temporal lobe epilepsy. *The European journal of neuroscience* 18, 2792-2802 (2003).

7 Kral, T. *et al.* Preoperative evaluation for epilepsy surgery (Bonn Algorithm). *Zentralblatt fur Neurochirurgie* 63, 106-110, doi:10.1055/s-2002-35826 (2002).

8 Pernhorst, K. *et al.* Promoter variants determine gamma-aminobutyric acid homeostasis-related gene transcription in human epileptic hippocampi. *Journal of neuropathology and experimental neurology* 70, 1080-1088, doi:10.1097/NEN.0b013e318238b9af (2011).

9 Schafer, J. & Strimmer, K. An empirical Bayes approach to inferring large-scale gene association networks. *Bioinformatics* 21, 754-764, doi:bti062 [pii] 10.1093/bioinformatics/bti062 (2005).

10 Opgen-Rhein, R. & Strimmer, K. From correlation to causation networks: a simple approximate learning algorithm and its application to high-dimensional plant gene expression data. *BMC Syst Biol* 1, 37, doi:10.1186/1752-0509-1-37 (2007).

11 Efron, B. Large-scale simultaneous hypothesis testing: the choice of a null hypothesis. *J. Am. Statist. Assoc* 99, 96-104 (2004).

12 Dittrich, M. T., Klau, G. W., Rosenwald, A., Dandekar, T. & Muller, T. Identifying functional modules in protein-protein interaction networks: an integrated exact approach. *Bioinformatics* 24, i223-231, doi:10.1093/bioinformatics/btn161 (2008).

13 Beisser, D., Klau, G. W., Dandekar, T., Muller, T. & Dittrich, M. T. BioNet: an R-Package for the functional analysis of biological networks. *Bioinformatics* 26, 1129-1130, doi:10.1093/bioinformatics/btq089 (2010).

14 Cline, M. S. *et al.* Integration of biological networks and gene expression data using Cytoscape. *Nat Protoc* 2, 2366-2382, doi:10.1038/nprot.2007.324 (2007).

15 Li, M., Wang, J. & Chen, J. A fats agglomerate algorithm for mining functional modules in protein interaction networks. in *International Conference on BioMedical Engineering and Informatics.* Sanya, Hainan, China, Vol. I, pp 3-7 (2008)

16 Scheet, P. & Stephens, M. A fast and flexible statistical model for large-scale population genotype data: applications to inferring missing genotypes and haplotypic phase. *Am J Hum Genet* 78, 629-644, doi:10.1086/502802 (2006).

17 Carlson, C. S. *et al.* Selecting a maximally informative set of single-nucleotide polymorphisms for association analyses using linkage disequilibrium. *Am J Hum Genet* 74, 106-120, doi:10.1086/381000 (2004).

18 Mardia, K. V., Kent, J. T. & Bibby, J. M. *Multivariate Analysis*. (Academic Press, Lodon, 1979).

19 Mei, H. *et al.* Principal-component-based multivariate regression for genetic association studies of metabolic syndrome components. *BMC genetics* 11, 100, doi:10.1186/1471-2156-11-100 (2010).

20 Bottolo, L. & Richardson, S. Evolutionary Stochastic Search for Bayesian model exploration. (2010).

21 Bottolo, L. *et al.* ESS++: a C++ objected-oriented algorithm for Bayesian stochastic search model exploration. *Bioinformatics* 27, 587-588, doi:10.1093/bioinformatics/btq684 (2011).

22 Petretto, E. *et al.* New insights into the genetic control of gene expression using a Bayesian multi-tissue approach. *PLoS Comput Biol* 6, e1000737, doi:10.1371/journal.pcbi.1000737 (2010).

23 Chen, W., Ghosh, D., Raghunathan, T. E. & Sargent, D. J. A false-discovery-rate-based loss framework for selection of interactions. *Statistics in medicine* 27, 2004-2021, doi:10.1002/sim.3118 (2008).

24 Bottolo, L. *et al.* Bayesian detection of expression quantitative trait Loci hot spots. *Genetics* 189, 1449-1459, doi:10.1534/genetics.111.131425 (2011).

25 Stephens, M. & Balding, D. J. Bayesian statistical methods for genetic association studies. *Nat Rev Genet* 10, 681-690, doi:10.1038/nrg2615 (2009).

26 Proposal for revised classification of epilepsies and epileptic syndromes. Commission on Classification and Terminology of the International League Against Epilepsy. *Epilepsia* 30, 389-399 (1989).

27 Berg, A. T. *et al.* Revised terminology and concepts for organization of seizures and epilepsies: report of the ILAE Commission on Classification and Terminology, 2005-2009. *Epilepsia* 51, 676-685, doi:10.1111/j.1528-1167.2010.02522.x (2010).

28 Patterson, N., Price, A. L. & Reich, D. Population structure and eigenanalysis. *PLoS Genet* 2, e190, doi:10.1371/journal.pgen.0020190 (2006).

29 Purcell, S. *et al.* PLINK: a tool set for whole-genome association and population-based linkage analyses. *Am J Hum Genet* 81, 559-575, doi:10.1086/519795 (2007).

30 Kasperaviciute, D. *et al.* Common genetic variation and susceptibility to partial epilepsies: a genome-wide association study. *Brain : a journal of neurology* 133, 2136-2147, doi:10.1093/brain/awq130 (2010).

31 Good, P. I. *Permutation, Parametric, and Bootstrap Tests of Hypotheses*. 3rd edn, (Springer, 2005).

32 Mazzuferi, M., Kumar, G., Rospo, C. & Kaminski, R. M. Rapid epileptogenesis in the mouse pilocarpine model: video-EEG, pharmacokinetic and histopathological characterization. *Exp Neurol* 238, 156-167, doi:10.1016/j.expneurol.2012.08.022 (2012).

33 Kim, D. *et al.* TopHat2: accurate alignment of transcriptomes in the presence of insertions, deletions and gene fusions. *Genome Biol* 14, R36, doi:10.1186/gb-2013-14-4-r36 (2013).

34 Robinson, M. D., McCarthy, D. J. & Smyth, G. K. edgeR: a Bioconductor package for differential expression analysis of digital gene expression data. *Bioinformatics* 26, 139-140, doi:10.1093/bioinformatics/btp616 (2010).

35 Behmoaras, J. *et al.* Genetic loci modulate macrophage activity and glomerular damage in experimental glomerulonephritis. *J Am Soc Nephrol* 21, 1136-1144, doi:10.1681/ASN.2009090968 (2010).

36 Seibenhener, M. L. & Wooten, M. W. Isolation and culture of hippocampal neurons from prenatal mice. *J Vis Exp*, doi:10.3791/3634 (2012).